

Integrating large language models and active inference to understand eye movements in reading and dyslexia

Francesco Donnarumma^a, Mirco Frosolone^a, and Giovanni Pezzulo^{a,*}

^aInstitute of Cognitive Sciences and Technologies, National Research Council, Via San Martino della Battaglia, 44, 00185, Rome, Italy

*Corresponding author. E- mail: giovanni.pezzulo@istc.cnr.it

August 10, 2023

Abstract

We present a novel computational model employing hierarchical active inference to simulate reading and eye movements. The model characterizes linguistic processing as inference over a hierarchical generative model, facilitating predictions and inferences at various levels of granularity, from syllables to sentences. Our approach combines the strengths of large language models for realistic textual predictions and active inference for guiding eye movements to informative textual information, enabling the testing of predictions. The model exhibits proficiency in reading both known and unknown words and sentences, adhering to the distinction between lexical and nonlexical routes in dual route theories of reading. Notably, our model permits the exploration of maladaptive inference effects on eye movements during reading, such as in dyslexia. To simulate this condition, we attenuate the contribution of priors during the reading process, leading to incorrect inferences and a more fragmented reading style, characterized by a greater number of shorter saccades. This alignment with empirical findings regarding eye movements in dyslexic individuals highlights the model’s potential to aid in understanding the cognitive processes underlying reading and eye movements, as well as how reading deficits associated with dyslexia may emerge from maladaptive predictive processing. In summary, our model represents a significant advancement in comprehending the intricate cognitive processes involved in reading and eye movements, with potential implications for understanding and addressing dyslexia through the simulation of maladaptive inference. It may offer valuable insights into this condition and contribute to the development of more effective interventions for treatment.

Keywords: Hierarchical active inference; Predictive coding; Large Language Models; Reading; Dyslexia

1 Introduction

Processing natural language - encompassing understanding, reading, and producing linguistic content - represents a fundamental ability of our species. Extensive research in psychology, neuroscience, linguistics, and machine learning has explored the intricate ways we process natural language.

Neuroscientific studies have revealed that natural language processing is inherently hierarchical, involving multiple brain regions and the integration of various sensory inputs [5, 4, 42]. This hierarchical processing spans from individual letters, phonemes, and words to complete sentence comprehension, with a hierarchy of brain areas actively maintaining these elements in working memory across multiple time scales [22].

Recent studies have increasingly supported the idea of *hierarchical predictive coding* as a formal theory describing perception as an inferential process, involving reciprocal exchanges between predictions and prediction errors across brain hierarchies [46, 15]. Several computational neuroimaging studies employing large language models (LLMs) during linguistic tasks have provided compelling evidence for both the predictive nature of language processing and the prediction hierarchies proposed by predictive coding [20, 48, 1, 53, 7, 6, 24].

Multiple lines of evidence strongly support the significance of prediction and hierarchical predictive coding in language processing. A recent computational neuroimaging study investigated human electrocorticographic (ECoG) responses to narratives using LLMs trained to predict the next word. Remarkably, the study revealed that like the LLMs, the brain engages in next-word prediction before word onset, computes prediction error signals, and utilizes latent representations of words (embeddings) contextualized based on the sequence of prior words [20].

Converging evidence emerges from three recent fMRI studies utilizing deep learning models during linguistic tasks. These studies not only confirm the predictive nature of language processing but also lend support to the prediction hierarchies proposed by predictive coding. The first fMRI study [48] trained a LLM to predict the next word at multiple time scales, identifying event boundaries as high surprise (also explored in [1, 53, 7]). Analyzing human functional magnetic resonance data during story listening, the study revealed an event-based hierarchy of surprise signals evolving along temporoparietal regions, with surprise signals gating bottom-up and top-down connectivity across neighboring time scales.

Furthermore, another fMRI study provided compelling evidence of the brain’s ability to predict a hierarchy of representations spanning multiple timescales in the future [6]. Enhancing LLMs with the capability to predict beyond the next word increased their fit with human data. The study also highlighted the hierarchical organization of brain predictions, ranging from temporal cortices predicting shorter-range representations (e.g., the next word) to frontoparietal cortices predicting higher-level, longer-range, and more contextual representations.

Notably, a separate fMRI study reported that evoked brain responses to words are influenced by linguistic predictions and a metric of unexpectedness, closely aligning with the hierarchical scheme of active inference, where lower-level predictions are informed by higher-level predictions [24]. Additionally, the study demonstrated that these hierarchical predictions can be well-aligned with standard levels of analysis in psycholinguistics, including meaning, grammar, words, and speech sounds, reinforcing the validity of the standard decomposition.

Taken together, these studies, alongside others [31, 51, 30, 52, 13], provide compelling support for the significance of prediction and hierarchical predictive coding in language processing. Moreover, they underscore the growing relevance of LLMs in comprehending linguistic processing [20].

Despite these advancements, the above studies have primarily focused on LLMs that passively receive sensory information, rather than actively searching for it. However, linguistic tasks, such as reading written text and listening to speech, are inherently active processes [12, 36, 19]. For example, during reading, eye movements (saccades) actively guide attention to relevant parts of the text, rather than processing every piece of text linearly. This active reading process suggests that saccades play a crucial role in hypothesis testing, selecting informative parts of the text to test predictions [12, 36, 11, 17].

Moreover, eye movement studies during reading have proven to be valuable in understanding reading difficulties, such as dyslexia. Dyslexia, a common reading disorder affecting 5-10% of the population, is associated not only with atypical brain activation patterns during language processing [42] but also with atypical eye movement patterns, such as increased numbers of forward saccades and decreased saccade lengths compared to control groups [54, 9, 32, 14].

The connection between prediction-based language processing and the perceptual challenges observed in dyslexia has been explored in previous studies like [28]. These investigations suggest that dyslexia could be characterized as a computational difficulty in effectively combining prior information, such as implicit memory of previous words, with noisy observations like the currently perceived word. Essentially, when prior information is given excessively low weighting relative to its internal noise, the time required to form a coherent understanding of text (or to perform auditory discrimination, as in [28]) significantly increases because novel observations consistently surprise dyslexics. Through computational simulations, the authors demonstrated that this pattern of results could account for dyslexics’ perceptual deficit. However, the proposed model lacks the capability to actively select information, such as generating saccades.

In this paper, we propose a novel computational model that unifies hierarchical predictive processing and hypothesis testing during reading by integrating the LLM BERT [10] with active inference [16, 39]. Our model views reading as an active (Bayesian) inference problem, employing a hierarchical generative model

to represent causal relationships between textual elements at different levels (letters, phonemes, words, and sentences). By generating predictions at each level and testing them through saccades, our model actively simulates reading.

The model incorporates three significant insights discussed earlier. Firstly, it conceptualizes linguistic processing as inference, employing a hierarchical generative model that allows for predicting and inferring at different timescales, such as syllables, words, and sentences. By integrating the powerful LLM BERT [10] at the highest hierarchical level, our model can handle realistic reading tasks effectively. Additionally, thanks to its hierarchical structure, our model can read text both word-by-word, a common approach in LLMs (i.e., the lexical route), and syllable-by-syllable, akin to the nonlexical route in dual route theories of reading [8].

Secondly, the model utilizes its generative capabilities not only for language recognition, similar to LLMs, but also for simulating eye movements and saccades. In our model, reading involves an active, hypothesis testing process: the model generates saccades to the most informative parts of the text to validate its predictions and disambiguate among competing hypotheses about the content being read [12, 36, 11, 17].

Thirdly, by reducing the influence of prior information in the inference [28], our model produces simulated eye movements during reading that align with empirical findings in dyslexia [54, 9, 26, 47]. This aspect allows the model to generate eye movement patterns consistent with dyslexic individuals’ reading impairments.

This model allows us to gain deeper insights into the integration of information during reading, the role of saccades in testing predictions, and the potential impact of maladaptive predictive processing in reading deficits associated with dyslexia. In the following sections, we demonstrate the model’s capabilities through simulations of word reading (*Simulation 1*), sentence reading (*Simulation 2*), reading unknown words and sentences (*Simulation 3*), and reading with prior information about the topic (*Simulation 4*).

2 Results

2.1 Brief explanation of the model

We present a novel hierarchical active inference model for reading and eye movements during reading [16]. Consistent with evidence of hierarchical language processing in the brain [24], our model consists of three levels representing syllables, words, and sentences, as illustrated in Fig. 1(a).

At each level, the inference process involves integrating three types of messages: bottom-up messages from nodes at the level below (conveying observations), top-down messages from nodes at the level above (conveying predictions), and lateral messages from nodes representing the previous timestep at the same level (providing memory). For instance, the inference about the current syllable is informed by bottom-up observations about the currently observed letter, top-down predictions from the currently inferred word, and lateral information about the previous syllable. Similarly, the inference about the current word relies on bottom-up observations (i.e., the currently estimated word), top-down predictions from the level above (i.e., at the sentence level), and information about the previous word.

To ensure that our model is capable of reading realistic text, we utilize the large language model BERT [10] to generate a probability distribution over the 100 most likely sentences consisting of 4-8 words. Importantly, this process can be iterated to read sentences of varying lengths, providing the flexibility to handle texts of different complexities.

Lastly, our model has the capability to determine where to make (forward or backward) saccades and select the next letter observation [11]. All three levels of the model are involved in the process of selecting where to direct the next saccade, by selecting the word (Level 3), syllable (Level 2), and letter (Level 1) to attend to. The selection is guided by considering the information gain of lexical elements at all levels, see Section 4 for further details.

Figure 1(b) visually represents the saccades generated by our model while reading an example sentence: *Active inference model of eye movements*. The model demonstrates uncertainty about the first word (*active*) and therefore reads it using two saccades to the first (*a*) and fourth (*i*) letters. It follows the same process for the subsequent two words (*inference* and *model*). However, at this stage, it skips the next two words, as

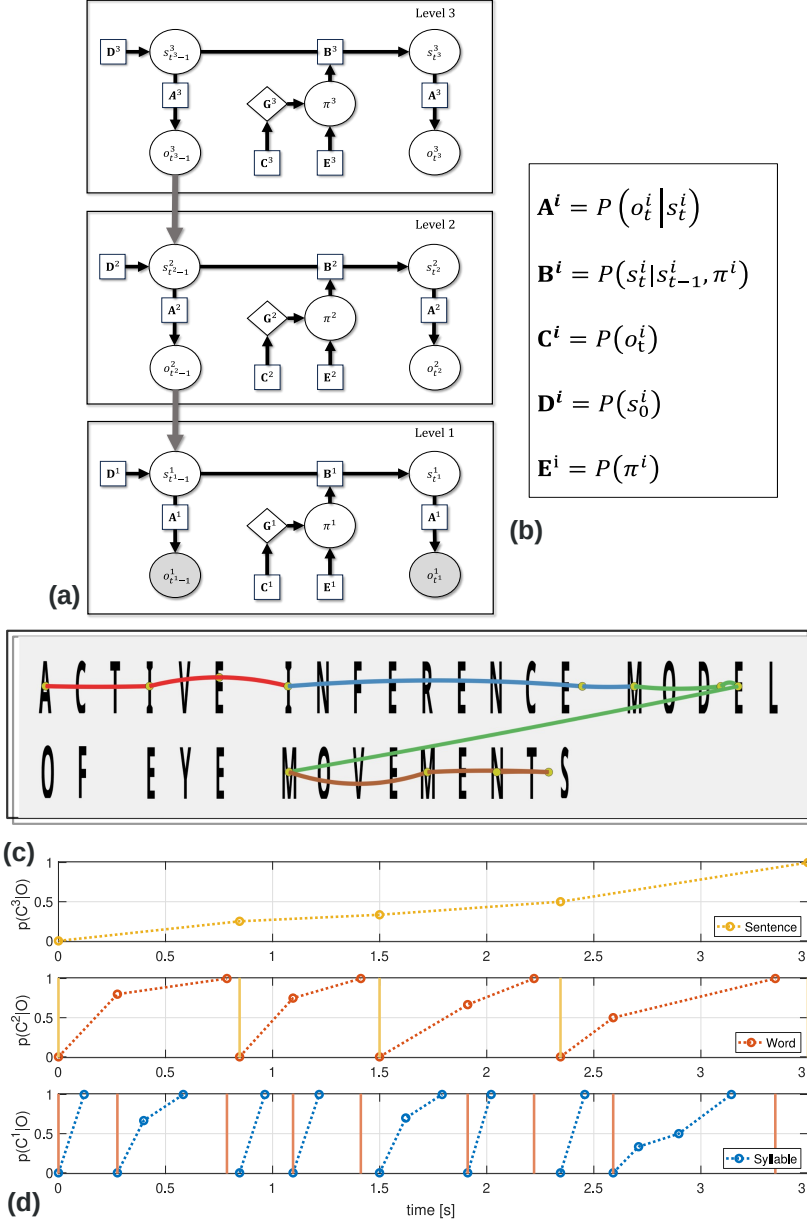


Figure 1: The hierarchical active inference model of reading and eye movements. (A) The hierarchical model comprises three layers for syllables, words, and sentences, represented using the formalism of Partially Observable Markov Decision Processes (POMDPs). Empty nodes indicate hidden variables, filled nodes represent observations, and edges depict probabilistic relations between the nodes, as detailed in B. (B) Model parameters. (C) The sequence of saccades generated by the model while reading an example sentence. Yellow dots indicate the positions of the saccades in the text, and colored lines trace the sequence of saccades from red to yellow. (D) Evolution of the probabilities of correctly recognized syllables (blue lines), words (red lines), and sentences (yellow lines) over time. The blue circles at the bottom level indicate saccades. Once the first level confidently infers a syllable (or when the maximum level of iterations is reached), it sends a bottom-up signal to the second level (indicated by the orange vertical bar) to aid in word inference. Similarly, the second level sends a signal to the third level (indicated by the yellow vertical bar) upon confidently inferring a word. Please refer to the main text for further explanation.

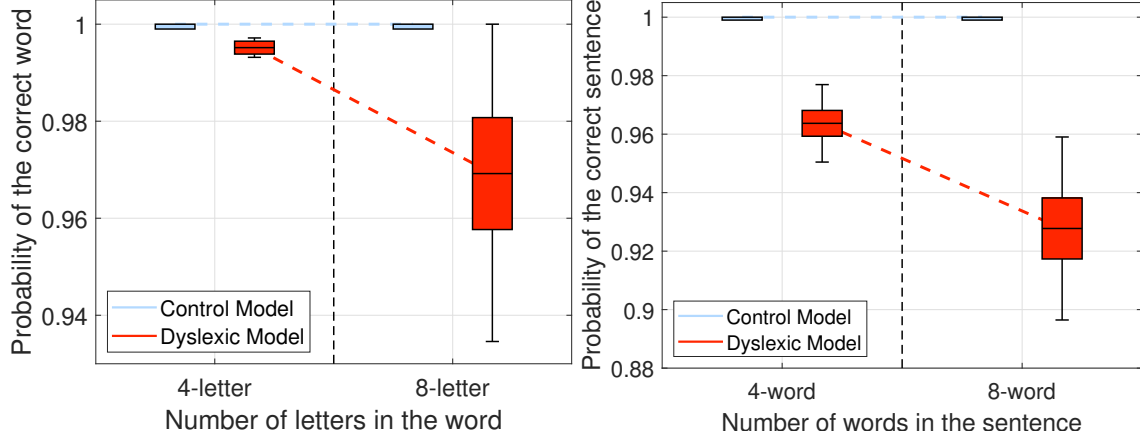


Figure 2: Results of Simulations 1 and 2: Probabilities assigned to the correct words. (a) Simulation 1: Probabilities assigned by the *Control model* (CM) and the *Dyslexic model* (DM) while reading 4-letter and 8-letter words. (b) Simulation 2: Probabilities assigned by the two models while reading 4-word and 8-word sentences. In this and the subsequent boxplots, the horizontal line represents the mean μ . The edges of the rectangle represent $\mu \pm \sigma$, where σ is the standard deviation of the mean. The area within the boxplot above the mean represents the interval between $\mu + \sigma$, while that below the red line represents the interval between $\mu - \sigma$. The vertical black lines limits extend within the range of $\mu \pm 3\sigma$.

it perceives the most informative word to be the one following (*movements*). This mechanism showcases the model’s ability to dynamically select the most relevant information during the reading process.

Figure 1(c) illustrates the probabilities of correctly recognized syllables (blue), words (red), and sentences (yellow) during the reading process. Over time, these probabilities approach one, indicating successful recognition. Additionally, the figure demonstrates that the levels operate at different time scales, with lower levels processing information more quickly than higher levels. This temporal separation arises because each level sends messages to the level above only after accumulating sufficient confidence (as shown by the vertical bars in the figure), a process that typically requires multiple rounds of inference [18].

2.2 Simulation 1: Reading single words

In this task, the objective is to read and recognize 100 words consisting of either 4 or 8 letters, selected from a pool of 726 words ranging from 1 to 8 letters, sourced from the BERT dictionary (see Tab. S.9 for the list of words). For ease of evaluation, each word is assigned the same a-priori probability of $1/726$ in the model.

The model’s performance is assessed using four metrics: word recognition accuracy, the probability assigned to the correct word, the number of saccades (forward, backward, or total), and their amplitude (i.e., the number of locations between letters). It is important to note that for this specific simulation, only levels 1 and 2 of the model are utilized, while Level 3 is not included.

Previous research has demonstrated that individuals with dyslexia exhibit a reading style characterized by more fragmented and laborious patterns, with a higher number of shorter saccades when reading words, and these difficulties are more pronounced with longer words [54, 33, 14]. To assess whether our model accurately replicates these findings, we compare two versions: (i) a *Control model* (CM) with no noise in its transition functions, allowing it to adequately consider the prior context during reading, and (ii) a *Dyslexic model* (DM), where we introduce noise in the transition functions of both the first (syllable) level and the second (word) levels, in line with the hypothesis that dyslexics struggle to integrate prior linguistic context [28].

The CM demonstrates perfect accuracy (100%), whereas the DM exhibits slightly lower accuracy for both 4-letter (99%) and 8-letter words (97%). Additionally, the CM assigns a 100% probability to the

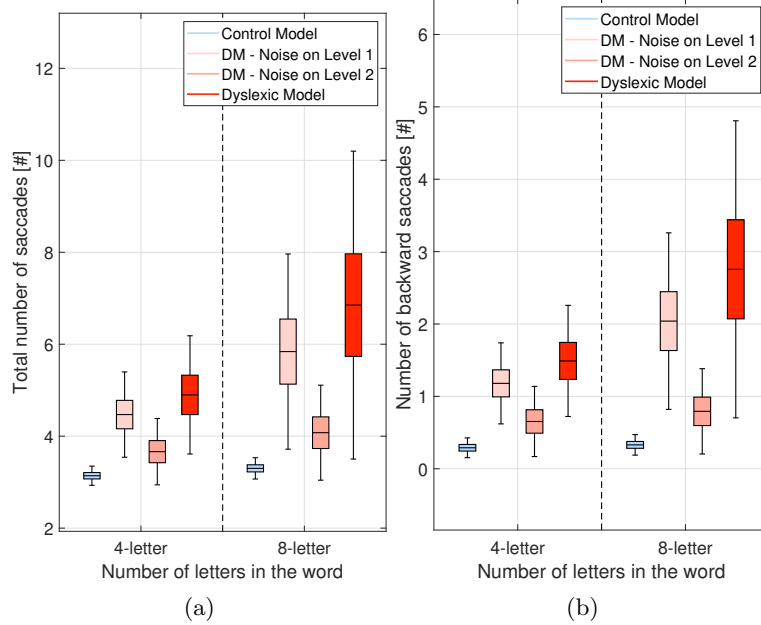


Figure 3: Simulation 1 results: Total number of saccades (a) and number of backward saccades (b) while reading 4-letter and 8-letter words. The figure compares the *Control Model* (*CM*) with no noise, the *Dyslexic Model* (*DM*) with noise at both hierarchical levels, and two versions of the *DM*, with noise only at the level of syllables (*DM - Noise on Level 1*) or words (*DM - Noise on Level 2*).

correct words, whereas the *DM* assigns a significantly lower probability to the correct word, especially for longer words. Please refer to Fig. 2(a) and Table S.1 for detailed results.

Moreover, the *DM* exhibits a significantly higher number of total saccades (Fig.3(a)) and backward saccades (Fig.3(b)) while reading both 4- and 8-letter words compared to the *CM*. Detailed statistical comparisons are available in Tab. S.2. To delve deeper into the impact of noise on eye movement dynamics during word reading, we created two variants of the *DM*, one with noise in the transition functions at the syllable level (*DM - Noise on Level 1*) and another with noise at the word level (*DM - Noise on Level 2*). This analysis reveals that noise at the first (syllable) level has a more significant effect than noise at the second (word) level.

In addition, the *DM* exhibits significantly shorter forward saccades (Fig.4(a)) but longer backward saccades (Fig.4(b)) while reading both 4- and 8-letter words in comparison to the *CM*. Detailed statistical comparisons are available in Table S.3.

In summary, our model successfully reproduces a wide range of empirical findings regarding how dyslexic individuals read single words, encompassing accuracy, reaction times, and eye movements. The lower probability assigned to words by the *DM* compared to the *CM*, as depicted in Fig.2(a), closely mirrors the results reported by Zoccolotti et al.[54], Fig.1(B). The accuracy results (Table S.1) are also consistent with the finding that dyslexic individuals fail to correctly read a small percentage of single words. Moreover, our simulations reveal that dyslexic individuals read significantly slower than controls [54, 37], as shown in Fig.1(A). This slower reading arises from the *DM* making more saccades than the *CM*, as illustrated in Fig. 3, with reading time being proportional to the number of saccades.

Furthermore, the results displayed in Fig. 4(a) closely match the finding that dyslexic individuals make shorter forward saccades compared to controls, particularly evident for longer words [33], Fig.4. Lastly, the results presented in Fig.4(b) closely resemble the finding that dyslexic individuals make significantly more and larger backward saccades than controls during reading [33], Fig. 5. Collectively, these outcomes demonstrate that our model effectively captures essential aspects of dyslexic reading behavior, providing

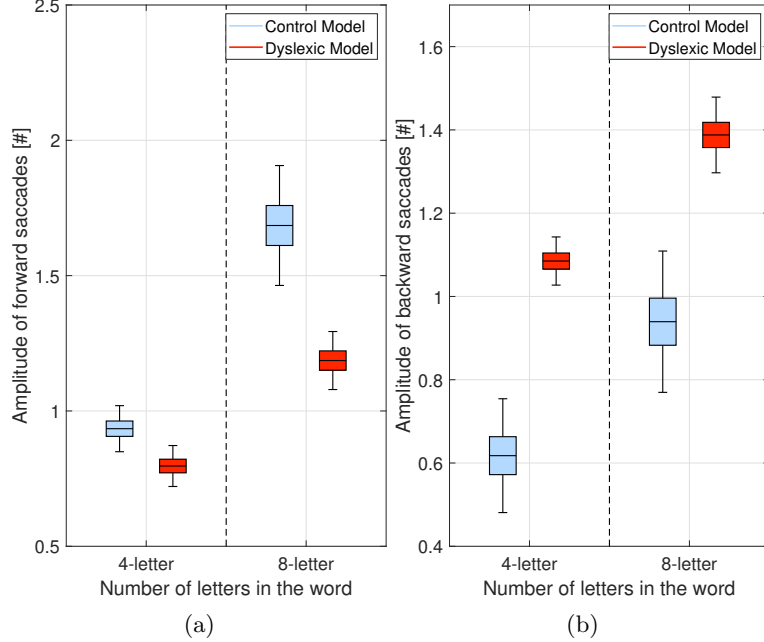


Figure 4: Simulation 1 results: Amplitude of forward (a) and backward (b) saccades while reading 4-letter and 8-letter words. The figure compares two models: the *Control Model* (CM) with no noise, and the *Dyslexic Model* (DM) with noise at both hierarchical levels.

valuable insights into the underlying mechanisms of dyslexia.

Significantly, our model offers a mechanistic understanding for all these observed findings, including the fragmented reading style of dyslexics. The DM’s shorter forward saccades stem from its poor contextual memory, making it less capable of predicting the next word efficiently. Consequently, it requires more saccades and time to read a text. Additionally, the increased need for backward saccades arises because the DM occasionally has to backtrack in the text to retrieve lost context. Moreover, our model readily explains why dyslexic reading impairments are more pronounced for longer words: noise in the transition function(s) accumulates over time, making reading longer words progressively more challenging. This comprehensive mechanistic explanation underscores the utility of our model in shedding light on the underlying cognitive processes contributing to dyslexia and its impact on reading behavior.

2.3 Simulation 2: Reading Sentences

This task involves reading and recognizing 100 sentences composed of 4 or 8 words, with each word consisting of 1 to 4 syllables, generated by BERT [10]. The sentences with 4 words have an average length of 25.96 ± 1.96 letters within the range of [21, 31]. Similarly, sentences with 8 words have an average length of 50.24 ± 1.64 letters, in the interval of [47, 55] (see Table S.8). To add complexity, we carefully selected sentences with a substantial word overlap (Table S.10). For this task, we utilize the comprehensive model depicted in Fig. 1, encompassing three hierarchical levels.

Previous studies have shown that proficient readers can scan lines of text using only a few saccades, while dyslexic individuals exhibit an increased number of shorter saccades [26, 47, 9] and fewer word skipping occurrences [3, 29, 23] compared to controls. Additionally, their performance decrease and increased number of saccades are influenced by the number of words in the text (see [9], Fig. 2). To verify whether our model accurately replicates these findings, we compare a *Control model* (CM) with no noise and a *Dyslexic model* (DM) with noise introduced in the transition functions of all three hierarchical levels.

Consistent with the empirical findings, the DM assigns significantly lower probabilities to the correct

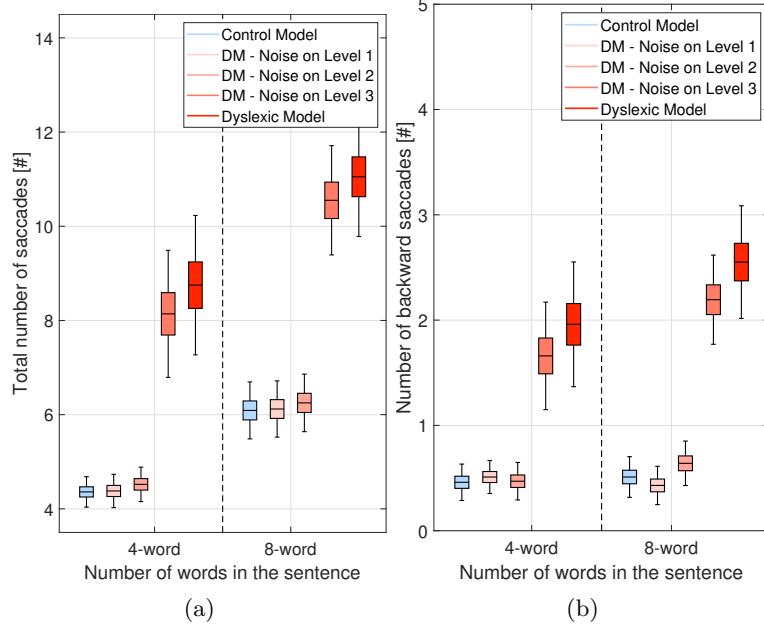


Figure 5: Simulation 2 results: Total number of saccades (a) and number of backward saccades (b) while reading 4-word and 8-word sentences. The figure compares the *Control Model* (*CM*) with no noise, the *Dyslexic Model* (*DM*) with noise at both hierarchical levels, and three alternative versions of the Dyslexic Model, where we added noise only at the level of syllables (*DM - Noise on Level 1*), words (*DM - Noise on Level 2*), or sentences (*DM - Noise on Level 3*).

sentences compared to the *CM*, and this effect is more pronounced for longer sentences (Fig. 2(b) and Table S.4). Additionally, the *DM* exhibits a significantly higher number of total saccades (Fig. 5(a-c)) and backward saccades (Fig. 5(b-d)) than the *CM* during sentence reading. When comparing different variants of the *DM* with noise introduced at various levels, we find that noise at the level of sentences has the most significant impact on impairing the reading performance.

Moreover, the *DM* exhibits significantly shorter forward saccades (Fig. 6(a)) and longer backward saccades (Fig. 6(b)) when reading both 4-word and 8-word sentences, in comparison to the *CM*. Detailed statistical comparisons can be found in Table S.6.

Collectively, these results build upon those observed for single words (Simulation 1) and successfully replicate empirical findings on dyslexic individuals' reading of sentences. The trends illustrated in Fig. 5(a) closely resemble the outcomes reported in Fig.3(A) of [9], which demonstrates that dyslexics make more saccades compared to controls while reading single lines of text (equivalent to reading 8-word sentences in Fig. 5(a)). Moreover, the number of saccades exhibited by the *DM* in our simulations aligns remarkably well with the numerical outcomes from the same study. Similarly, the outcomes in Fig. 6(a) closely resemble the findings depicted in Fig. 3(B) of [9], revealing that dyslexics make shorter forward saccades than controls. In this context, the amplitudes of both dyslexics and the *DM* model closely correspond.

In summary, our results effectively reproduce the observation that dyslexic individuals make a greater number of shorter saccades while reading sentences, and their reading performance is dependent on the number of words in the sentence (refer to [9], Fig.2). The causes of these impairments are akin to those discussed for single words (Simulation 1), but their effects become more pronounced as sentence comprehension necessitates the integration of information over more extended periods. For instance, the high occurrence of ample backward saccades is a result of the *DM* frequently losing context and subsequently needing to backtrack to the initial words of a sentence to regain it. This further clarifies why noise at the sentence level substantially impairs this task (Fig. 5).

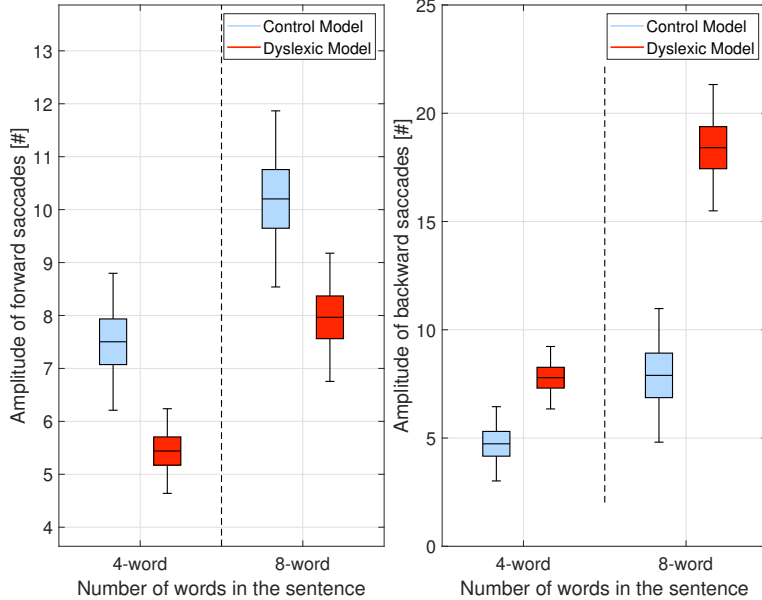


Figure 6: Simulation 2 results: Amplitude of forward (a) and backward (b) saccades while reading 4-letter and 8-letter words. The figure compares two models: the *Control Model (CM)* with no noise, and the *Dyslexic Model (DM)* with noise at both hierarchical levels.

2.4 Simulation 3. Reading novel words and sentences

Up to this point, our simulations involved reading *known* words and sentences, already present in the BERT vocabulary. Hence, the model could confidently assign probabilities at the second and third layers. Nevertheless, our model can also read *unknown* words and sentences, despite its inability to assign them a prior probability. When confronted with unknown words or sentences, the model reads syllable-by-syllable (or word-by-word) and simultaneously acknowledges uncertainty at the second (or third) level. This mode aligns with the nonlexical (or sublexical) route in dual-route theories of reading [8].

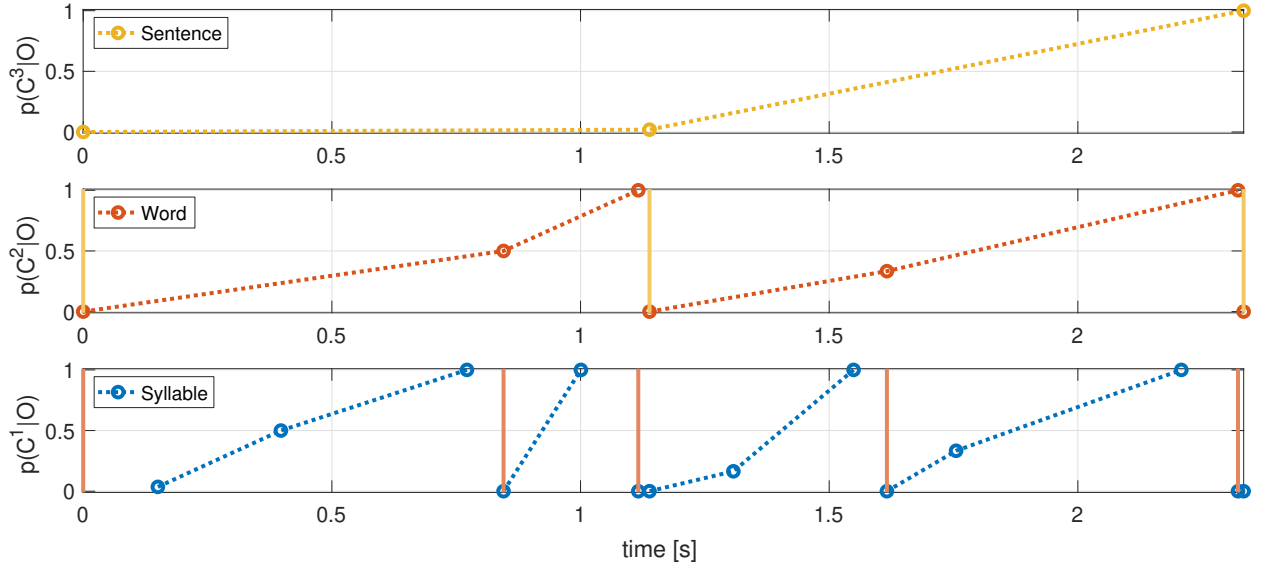
To demonstrate this capability, we simulate reading the last four words of the sentence *This paper is also framed in an offbeat manner* and compare two versions of the model: one in which all the words exist in the model’s vocabulary (Fig. 7(a)) and another where the word *offbeat* is absent from the vocabulary (Fig. 7(b)). In the version with all known words, the model behaves similarly to the previous simulations, accurately recognizing all the words and the sentence. This is evident in Fig. 7(a), where probabilities at the second and third levels quickly converge to one after a few iterations.

Conversely, the version without knowledge of the word *offbeat* repeatedly makes saccades to the syllables of this word (at Level 1) until it reaches the maximum number of iterations set for this simulation (here, $T_{\max}^3 = 6$). It correctly recognizes each syllable and can read the word aloud, potentially adding it to its vocabulary [8]. However, it does not recognize the word (at Level 2) or the sentence (at Level 3). This is evident in Fig. 7(b), where probabilities at the second and third levels never exceed 0.5.

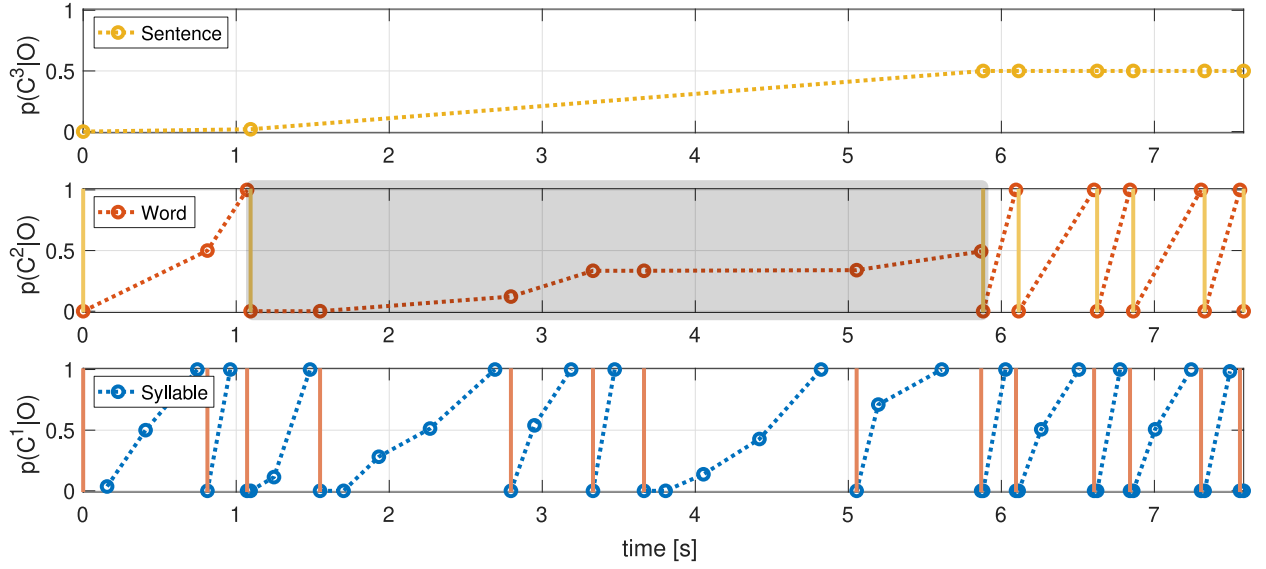
2.5 Simulation 4: Knowing the topic improves sentence recognition

In this section, we showcase another capability of the model that has not been discussed yet. The model can be enriched with *priors* regarding the linguistic topic at each hierarchical level, such as the *topic of the sentence* at the third level. This prior knowledge makes certain sentences a-priori more (or less) likely, thus expediting the recognition process if the context aligns correctly.

To illustrate this, we conduct a task involving the recognition of 100 sentences, each containing 9 words, generated by BERT. These sentences comprise an average of 69.55 ± 5.02 letters, ranging between 61 and 82



(a)



(b)

Figure 7: Simulation 3 results: Reading known vs. unknown words. Evolution of the probabilities of correctly recognized syllables (blue lines), words (red lines), and sentences (yellow lines) over time, while reading (a) known words or (b) the unknown word *offbeat*. The blue circles at the bottom level indicate saccades. The figure format is consistent with Fig. 1(d).

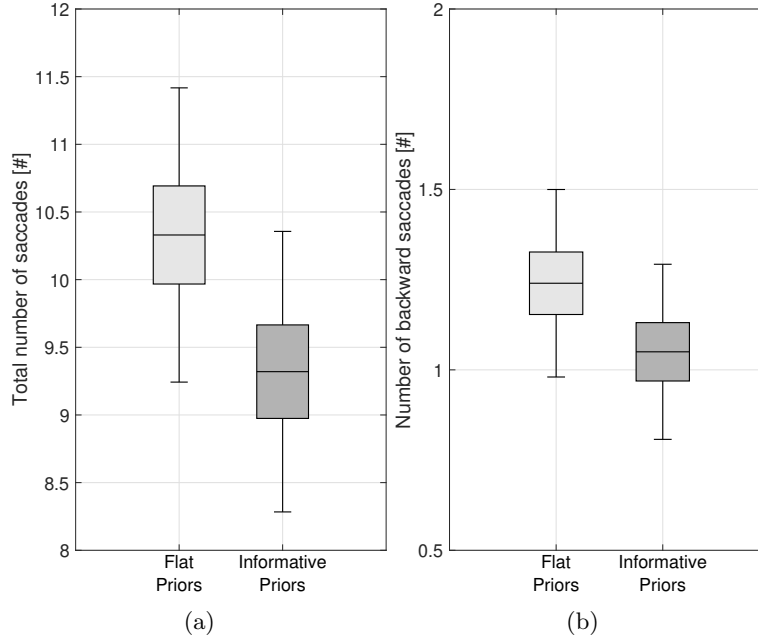


Figure 8: Simulation 4 results: How prior information affects the reading process. The figure displays the total saccades (a) and backward saccades (b) of two model versions: one with a flat prior about the topic of the text (flat prior) and another with certain knowledge of the topic (informative prior). The comparison highlights the impact of prior information on the number and nature of saccades during reading.

characters (see Table S.8). We allocate one-third of the sentences to each of the three topics of the European Research Council (ERC): Physical Sciences and Engineering (PE), Life Sciences (LS), and Social Sciences and Humanities (SH).

We compare the performance of two versions of the model: one with a *flat prior* (33.3%) regarding the sentence being read, and another with an *informative prior* that assigns a probability of 100% to the correct topic. As depicted in Fig. 8, the model with an informative prior requires significantly fewer total saccades and backward saccades than the model with a flat prior (see Table S.7 for statistical comparisons). This advantage arises because knowing the topic allows the model to predict certain words with high confidence, enabling it to skip unnecessary saccades during the reading process. Intriguingly, despite the model with an *informative prior* skipping several words, it does not necessitate more backward (corrective) saccades compared to the model with a *flat prior*. This indicates that the prior information promotes a better speed-accuracy trade-off.

3 Discussion

In this paper, we presented a novel hierarchical active inference model of reading, which combines the robust generative abilities of large language models [10, 44] with the inferential and information-gathering capacities of active inference [16, 39].

Large language models, like BERT (Bidirectional Encoder Representations from Transformers) [10] and GPT (Generative Pre-trained Transformer) [44], have demonstrated remarkable performance in various natural language processing tasks, including question answering, language translation, text classification, and sentence prediction. These models can learn essential linguistic structures without external supervision, making them valuable tools to explore language processing in the brain [35, 20]. However, they lack the *active* strategies employed by human readers, such as the ability to make saccades selectively on the most

informative parts of the text [12, 36].

To capture active reading, we integrate BERT [10] into a hierarchical active inference framework [16, 39]. Active inference is a theoretical framework that describes how the brain employs probabilistic inference over a generative model to effectively sample sensory inputs, minimizing variational free energy or prediction errors. For modeling reading, we utilize a hierarchical generative model, aligning with evidence suggesting that language processing in the brain operates through hierarchically organized predictions and prediction errors [48, 6, 24].

By placing BERT at the top of the hierarchy, we ensure accurate next-word predictions and the model’s capability to tackle real-world reading tasks. Beyond next-word prediction, our hierarchical model facilitates both inferring the content being read and predicting future elements across different linguistic levels, such as syllables, words, and sentences. Our simulation results demonstrate the model’s perfect accuracy in inferring words (Simulation 1) and sentences (Simulation 2) during reading. Additionally, this hierarchical structure enables the model to read novel words not present in BERT’s vocabulary (Simulation 3), assembling them syllable-by-syllable, representing the nonlexical (or sublexical) route in dual route theories of reading [8]. Moreover, the model can incorporate prior knowledge, like the topic of the sentence, to expedite the reading process (Simulation 4). Significantly, the model offers interpretability through its alignment of distinct levels with established linguistic constituents (sentences, words, syllables), which could correspond to distributed neural populations or cell assemblies within the brain [24, 43]. While delving into the neural mechanisms that underlie this proposed framework extends beyond the confines of this article, future studies could encompass the simulation of neuronal dynamics during the inference process, in terms of variational free energy minimization [18, 27].

Using active inference, our model characterizes reading as an *active*, hypothesis testing process, allowing us to simulate eye movements during reading. The core idea is that saccades are directed to the most informative parts of the text, enabling the model to test its predictions and reduce uncertainty about the text being read [12, 36, 11, 17]. Remarkably, this *epistemic* objective, aimed at uncertainty reduction, emerges naturally from active inference, as explained in Section 4. In summary, our model offers a comprehensive account of prediction-based written text processing, involving hierarchical inference of the content being read, prediction of upcoming textual elements, and active testing of predictions through saccades, which, in turn, inform further inference.

Importantly, our model also enables the modeling of abnormal eye movements observed in reading disorders, such as dyslexia [34, 25, 42]. Our simulations replicate the empirical findings that dyslexics, compared to controls, exhibit fragmented text processing, characterized by an increased number of shorter saccades, both while reading single words (Simulation 1) and sentences (Simulation 2) [54, 9, 26, 47]. Interestingly, our model attributes these reading deficits to a straightforward mechanism: an attenuation of the role of prior information during inference [28]. By introducing noise in the model’s transition functions, we impair its working memory of previous inference phases, forcing it to repeatedly gather evidence. Considering the cumulative effect of noise on the inference process, this mechanism accounts for why perceptual deficits in dyslexics become more pronounced for longer words and sentences [54, 9]. To summarize, the model provides a mechanistic explanation of reading disorders in dyslexia, aligning well with prediction-based theories of language processing and reading.

However, it is crucial to note that dyslexia is highly heterogeneous, and its underlying causes are still heavily debated [40, 55, 45, 49, 50]. While the attenuation of priors [28] explored in this article may not account for all aspects of dyslexia, our model is easily extendable to incorporate other (non-alternative) mechanisms that could contribute to reading impairments. For instance, various proposals point to disorders of low-level information sampling and attention shifting [21], or a visual attention span disorder characterized by a reduction in the number of letters that can be processed in parallel [41]. These proposals (and others) can be readily integrated into the model by modifying the likelihood function that maps letters to syllables, as described in Section 4. Future research could utilize the presented model to compare alternative proposals side-by-side, shedding light on the mechanisms of dyslexia and other reading difficulties, and informing the development of effective interventions to improve reading skills.

4 Methods

Here, we provide a brief introduction to active inference (see [39] for details) and then we illustrate the hierarchical active inference reading model used in this paper.

4.1 Brief introduction to Active Inference

Active Inference is a framework that models an agent’s action-perception loop by minimizing variational free energy [39]. The key objective is to minimize free energy, and to achieve this, the agent possesses a generative model (like the one illustrated in Fig.1), which captures the joint probability of the stochastic variables (hidden states and observations) using the formalism of probabilistic graphical models[2]. The agent’s perception involves making inferences about the hidden states based on the observed sensory inputs, while action involves selecting actions that can change the hidden states and optimize the model’s predictions. The generative model for active inference is defined as follows:

$$P(o_{0:K}, s_{0:K}, u_{1:K}, \gamma | \Theta) = P(\gamma | \Theta) P(\pi | \gamma, \Theta) P(s_0 | \Theta) \prod_{t=0}^K P(o_t | s_t, \Theta) P(s_{t+1} | s_t, \pi_t, \Theta) \quad (1)$$

where

- $P(o_t | s_t, \Theta) = \mathbf{A}$,
- $P(s_{t+1} | s_t, \pi_t, \Theta) = \mathbf{B}(u_t = \pi_t)$,
- $P(\pi_t | \gamma, \Theta) = \sigma(\ln \mathbf{E}\gamma \cdot \mathbf{G}(\pi_t) | \Theta)$,
- $P(\gamma, \Theta) \sim \Gamma(\alpha, \beta)$, and
- $P(s_0 | \Theta) = \mathbf{D}$.

The set $\Theta = \{\mathbf{A}, \mathbf{B}, \mathbf{C}, \mathbf{D}, \mathbf{E}, \alpha, \beta\}$ parametrizes the generative model:

- The (likelihood) matrix \mathbf{A} encodes the relations between the observations \mathbf{O} and the hidden causes of observations \mathbf{S} .
- The (transition) matrix \mathbf{B} defines how hidden states evolve over time t , as a function of a control state (action) u_t ; note that a sequence of control states $u_1, u_2, \dots, u_t, \dots$ defines an *action policy* (or *policy* for short) π_t .
- The matrix \mathbf{C} is an a-priori probability distribution over observations (and typically encodes the agent’s preferences).
- The matrix \mathbf{D} is the prior belief about the initial hidden state, before receiving any observation.
- \mathbf{E} encodes a prior over the policies (reflecting habitual components of action selection).
- $\gamma \in \mathbb{R}$ is a *precision* that regulates action selection and is sampled from a Γ distribution, with parameters α and β .

In active inference, the process of perception involves estimating hidden states based on observations and previous hidden states. At the start of the simulation, the model has access to an initial state estimate s_0 through \mathbf{D} and receives an observation o_0 that helps refine the estimate by using the likelihood matrix \mathbf{D} . Subsequently, for each time step $t = 1, \dots, K$, the model infers its current hidden state s_t by considering the transitions determined by the control state u_t , as specified in \mathbf{B} . Active inference employs an approximate posterior over (past, present, and future) hidden states and parameters $(s_{0:K}, u_{1:K}, \gamma)$. This approach utilizes

a factorized form of variational inference, which corresponds to a framework developed in physics known as mean field theory [38]. Using a mean field approximation, namely assuming that all variables are independent, the factorized approximated posterior can be expressed as:

$$Q(s_{0:K}, u_{1:K}, \gamma) = Q(\pi) Q(\gamma) \prod_{t=0}^K Q(s_t | \pi_t) \quad (2)$$

where the sufficient statistics are encoded by the expectations $\mu = (\tilde{s}^\pi, \pi, \gamma)$, with $\tilde{s}^\pi = \tilde{s}_0^\pi, \dots, \tilde{s}_K^\pi$. Following a variational approach, the distribution in (2) best approximates the posterior when its sufficient statistics μ minimise the free energy of the generative model, see [39]. This condition holds when the sufficient statistics are:

$$s_t^\pi \approx \sigma(\ln \mathbf{A} \cdot o_t + \ln(\mathbf{B}(\pi_{t-1}) \cdot s_{t-1}^\pi)) \quad (3a)$$

$$\pi = \sigma(\ln \mathbf{E} - \gamma \cdot \mathbf{G}(\pi_t)) \quad (3b)$$

$$\gamma = \frac{\alpha}{\beta - \mathbf{G}(\pi)} \quad (3c)$$

Action selection in the active inference framework involves choosing a policy, represented by a sequence of control states u_1, u_2, \dots, u_t , that is expected to minimize free energy most effectively in the future. The policy distribution π is defined by the Softmax function $\sigma(\cdot)$ and the *expected free energy (EFE)* of the policies, denoted by \mathbf{G} . The EFE incorporates goal-directed components of action selection. Additionally, the precision term γ plays a role in encoding the confidence of beliefs concerning \mathbf{G} .

The EFE $\mathbf{G}(\pi_t)$ of each policy π_t is defined as:

$$\mathbf{G}(\pi_t) = \sum_{\tau=t+1}^K D_{KL}[Q(o_\tau | \pi) \parallel P(o_\tau)] + \mathbb{E}_{\tilde{Q}}[H[P(o_\tau | s_\tau)]] \quad (4)$$

where $D_{KL}[\cdot \parallel \cdot]$ and $H[\cdot]$ are, respectively, the Kullback-Leibler divergence and the Shannon entropy, $Q(o_\tau, s_\tau | \pi) \triangleq P(o_\tau, s_\tau) Q(s_\tau | \pi)$ is the predicted posterior distribution, $Q(o_\tau | \pi) = \sum_{s_\tau} Q(o_\tau, s_\tau | \pi)$ is the predicted outcome, $P(o_\tau)$ is a categorical distribution representing the preferred outcome and encoded by \mathbf{C} , and $P(o_\tau | s_\tau)$ is the likelihood of the generative model encoded by the matrix \mathbf{A} .

The EFE in (4) can be used as a quality score for the policies and has two terms:

- *Expected Cost.* The first term of (4) is the Kullback-Leibler divergence between the (approximate) posterior and prior over the outcomes and it constitutes the *pragmatic* (or utility-maximizing) component of the quality score. This term favours the policies that entail low risk and minimise the difference between predicted ($Q(o_\tau | \pi)$) and preferred ($P(o_\tau) \equiv \mathbf{C}$) future outcomes.
- *Expected Ambiguity.* The second term of (4) is the expected entropy under the posterior over hidden states and it represents the *epistemic* (or uncertainty-minimizing) component of the quality score. This term favours policies that lead to states that diminish the uncertainty future outcomes $H[P(o_\tau | s_\tau)]$.

After scoring all the policies using the EFE, action selection is performed by drawing over the action posterior expectations derived from the sufficient statistic π computed via (3b). Then, the selected action is executed, the model receives a novel observation and the perception-action cycle starts again. See [39] for more details.

4.2 Hierarchical Active Inference model for reading

The active inference model employed in this study is structured hierarchically, consisting of three levels denoted by $i \in 1, 2, 3$ in our simulations. At each level, the model encodes hidden variables associated with different aspects of textual content: syllables at Level 1, words at Level 2, and sentences at Level 3.

This hierarchical organization allows the model to effectively capture and process information at multiple linguistic scales, enabling the inference and generation of syllables, words, and sentences during the reading process. For a visual representation of the model’s architecture, refer to Fig. 1(a-b).

The hidden states of each level are obtained by the tensorial product: $S^{(i)} = C^{(i)} \otimes L^{(i)} \otimes T^{(i)}$ among three factors:

- the *Content* $C^{(i)}$, i.e., the textual content proper: *Syllable*, *Word* or *Sentence*,
- the *Location* $L^{(i)}$, i.e. the position of a portion of the textual content (Location of the Letter in the syllable, Location of the Syllable in the word, and Location of the Word in the Sentence), thus corresponding to a $C^{(i-1)}$ -type content of the next lower level if $i > 1$ or to location of a *Letter* in a *Syllable* if $i = 1$.
- the *Topic* $T^{(i)}$, i.e. the context to which each *Content* variable is associated. Please note that we only use this factor in Simulation 4; in the other simulations, we remove it.

The Content is the crucial element of the chain: it is the text that is obtained from the recursive concatenation of the elements from the level below. A *Syllable* is a concatenation of $N^{(1)}$ *Letters* $c^{(0)}$ (which are not hidden states but observations, belonging to a finite *Alphabet* $C^{(0)}$, see below). A *Word* is a concatenation of $N^{(2)}$ syllables $c^{(1)}$ belonging to the set of *Syllables* $C^{(1)}$ and a *Sentence* is concatenation of $N^{(3)}$ *Words* $c^{(2)}$ belonging to the set $C^{(2)}$. In general, the i -th content $c^{(i)} \in C^{(i)}$ is a concatenation of $N^{(i)}$ sub-contents $c_n^{(i-1)} \in C^{(i-1)}$ such that

$$c^{(i)} = c_1^{(i-1)}, \dots, c_{N^{(i)}}^{(i-1)}$$

The observations $O^{(i)} = O_1^{(i)} \otimes O_2^{(i)} \otimes O_3^{(i)}$ consists of the tensorial product among:

- the observation $O_1^{(i)}$ of the content of the level below $C^{(i-1)}$. Note that only Level 1 of the model receives an actual textual observation: namely, a letter $c^{(0)}$ belonging to the Alphabet $C^{(0)}$. The other two levels receive as observations the content at the level below: the observations at levels 2 and 3 are the inferred syllables and words, respectively;
- the observation $O_2^{(i)}$ corresponding to the location $L^{(i)}$ of the $C^{(i-1)}$ content;
- the feedback response $r \in O_3^{(i)}$, (“correct” or “wrong”) that inform the model whether the current content $C^{(i)}$ belongs to the correct or wrong topic. This observation is only useful in Simulation 4, in which we consider models with or without prior information about the topic.

The likelihood mapping $p(O^{(i)}|S^{(i)})$ between hidden states $S^{(i)}$ and observations $O^{(i)}$ is specified through the tensor $\mathbf{A}^{(i)}$, defined as the tensorial product $\mathbf{A}^{(i)} = A_1^{(i)} \otimes A_2^{(i)} \otimes A_3^{(i)}$ where

- $A_1^{(i)}$ is a 4-order tensor mapping the hidden states $S^{(i)}$ (3-order tensors) to the observation $O_1^{(i)}$ corresponding to the content $C^{(i-1)}$ if $i > 1$ or to the observation of a letter if $i = 1$; In our simulations, this probability is typically an identity matrix: the probability of observing content $c^{(i)}$ if the reader agent is in the corresponding location $l^{(i)}$ is set to 1. Note that it would be easy to extend the model to cover perceptual deficits or poor familiarity with words, by simply adding noise in the likelihood function.
- $A_2^{(i)}$ is a 4-order tensor mapping the hidden states $S^{(i)}$ to observation $O_2^{(i)}$ corresponding to the locations $L^{(i)}$; Also in this case we assume no noise, so the probability of observing a given location when the reader agent eye point to that location is set to 1.
- $A_3^{(i)}$ is a 4-order tensor mapping the hidden states $S^{(i)}$ to the feedback response in $O_3^{(i)}$. In our simulation we adopt a binary probability in our simulation: the likelihood is set to 1 if the content belongs to the correct topic and to 0 otherwise.

The mapping $p\left(s^{(i)}|s_{t-1}^{(i)}, \pi_t\right)$ between hidden states given the control state u is specified by the tensor $\mathbf{B}^{(i)}$, defined as the tensorial product $\mathbf{B}^{(i)} = B_1^{(i)} \otimes B_2^{(i)} \otimes B_3^{(i)}$ where

- $B_1^{(i)}$ maps the transition between content states at successive time steps. Note that in our simulations, we use transitions models without noise (for the *control model*) and with noise added at one or more hierarchical levels (for the *dyslexic models*). For this, when we formalize the mapping $p\left(c_t^{(i)}|c_{t-1}^{(i)}, \pi_t\right) = \delta^{(i)}$ we use a modulating factor $\delta^{(i)}$, which we set to 1 in the case without noise and to a number below 1 in the case with noise. Noise implies that the prior knowledge about (or the working memory) of the content variable fades away during reading – requiring more evidence and more saccades to solve the reading tasks.
- $B_2^{(i)}$ maps the transitions between locations. We equip the model with the probability $p\left(l_t^{(i)}|l_{t-1}^{(i)}, \pi_t\right)$ to jump from one location to another, without noise (i.e., the act of jumping to the selected location is executed with no errors). While in principle one can jump to any location, here we restrict the jump possibilities, by setting priors over locations D and policies E , see below.
- $B_3^{(i)}$ maps the probability $p\left(tp_t^{(i)}|tp_{t-1}^{(i)}, \pi_t\right)$ to jump from one topic to another. We consider this transition to be noiseless. This action is only relevant in Simulation 4, in which we compare the model with or without prior information about the topic.

The tensor $\mathbf{C}^{(i)} = C_1^{(i)} \otimes C_2^{(i)} \otimes C_3^{(i)}$ encodes the priors over the observations that encode preferred outcomes:

- $C_1^{(i)}$, prior preferences on the outcomes $O_1^{(i)}$, (e.g. for Level 3 encoding sentences, prior on expected words);
- $C_2^{(i)}$, prior preferences on the outcomes $O_2^{(i)}$ (e.g. for Level 3 encoding sentences, prior on expected word locations)
- $C_3^{(i)}$, prior preferences on the outcomes $O_3^{(i)}$ (e.g. for Level 3 encoding sentences, prior on expected sentence topic).

The tensor $\mathbf{D}^{(i)} = D_1^{(i)} \otimes D_2^{(i)} \otimes D_3^{(i)}$ encodes the priors over the hidden states:

- $D_1^{(i)}$, priors over the *Content* at the corresponding level. It corresponds to the initial distribution of the content variable (e.g. at Level 3, it is the prior over the initial sentence distribution). For simplicity, here we use flat priors. However, it is possible to use this feature to model the fact that syllables, words and sentences have different frequencies.
- $D_2^{(i)}$, priors on the *Locations*. For simplicity, here we assign a very high prior to the first element of the content, following the assumption that people start reading (for example) a word from the first syllable. During reading, after each loop the $D_1^{(3)}$ is initialized to the next word not yet read.
- $D_3^{(i)}$, priors on the *Topics*. We only use this feature in Simulation 4, in which we show that having prior information about the topic of the sentence can speed up its reading. In all the other simulations, we set flat priors over Topics.

The matrix $\mathbf{E}^{(i)}$ encodes the priors over the policies.

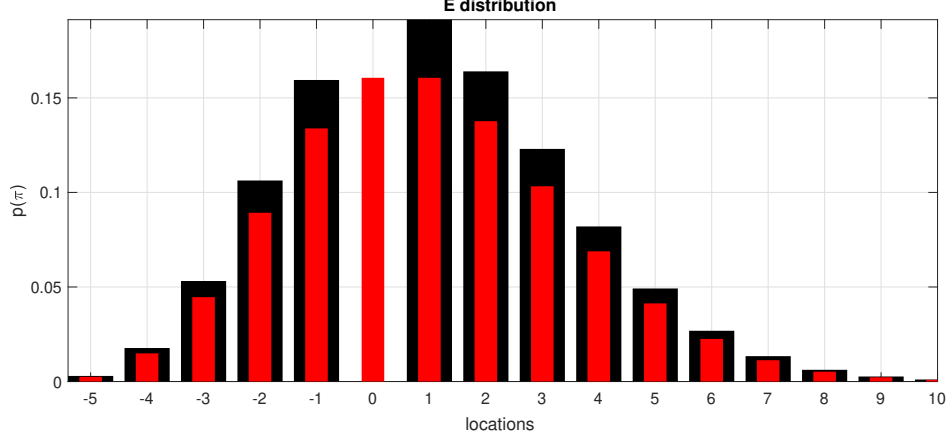


Figure 9: Priors on the policies that make transitions between word locations at Level 3 of the generative model. We first set the prior as a Poisson distribution with $\lambda = 6$ (red bars), centered on the current location (i.e., the value of the maximum of the distribution is in 0). We next set the probability of reading the same word two consecutive times to zero and re-normalize the distribution, leading to the distribution shown by the black bars.

4.3 Saccade selection

Saccade selection arises from a competition among policies spanning all hierarchical levels, determining the location of the next word in the sentence (Level 3), syllable in the word (Level 2), and letter in the syllable (Level 1). The number of policies at each level varies depending on the simulation. For example, when reading 8-word sentences in Simulation 2, the model uses 8 policies to jump among words, 4 policies to jump among syllables and 5 policies to jump among letters.

Policy selection considers the Expected Free Energy (EFE) described in (4). However, within the simulations detailed in this study, we employ flat prior preferences (denoted as C), resulting in policy selection that solely weighs the information gain associated with the following word, syllable, or letter.

Furthermore, policy selection considers the prior distribution over policies (denoted as E). Our simulations adopt flat priors for Level 1 ($E^{(1)}$) and Level 2 ($E^{(2)}$), signifying no inherent constraints on transitioning between letters within a syllable or between syllables within a word. To discourage overly long saccades, a finite moving window for favored transitions among word locations is set for Level 3 ($E^{(3)}$). This is achieved through a Poisson distribution $Pois(\lambda)$, where λ equals 6 (as displayed in Fig. 9, depicted by red bars). Additionally, the probability of reading the same word consecutively is set to zero, resulting in the normalization of the distribution. This culminates in the distribution depicted by the black bars in Fig. 9.

4.4 Explanation of the example in Fig. 1

Fig. 10 presents a schematic illustration of the textual elements inferred by the model while reading the sentence "Active inference model of eye movements" as depicted in Fig. 1. The diagram distinguishes between two factors of the generative model – Content and Location – illustrated by the left and right trees, respectively. The left (content) tree in Fig. 10 demonstrates that the model infers the first word "active" at Level 2 by examining the letter "a". This, in turn, leads to the inference of the syllable "ac" at Level 1, followed by the letters "t" and "e", enabling the inference of the syllable "tive" at Level 2. The right (location) tree in Fig. 10 shows the respective locations of these three letters "a", "t", and "e" within their syllables at Level 1, and the positions of "ac" and "tive" within the word at Level 2. This process continues for the subsequent words (excluding "of" and "eye", which are skipped during reading, as seen in Fig. 10), until the entire sentence is recognized.

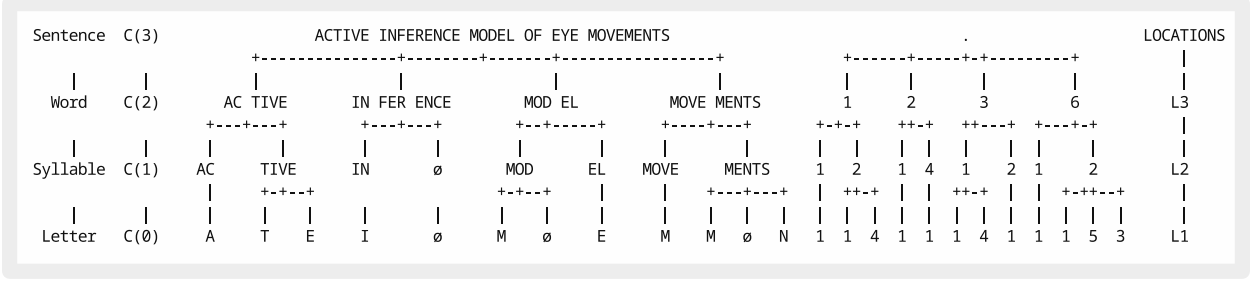


Figure 10: Graphical explanation of the model’s reading process for the example sentence ”Active inference model of eye movements” introduced in Fig. 1. The figure illustrates the distinction between two factors of the generative model: content (left tree) and location (right tree). Refer to the main text for a detailed explanation.

4.5 Explanation of the example in Fig. 7

The example in Fig. 7 illustrates the distinction between reading a known versus a novel word and the termination conditions for inference at each hierarchical level. The inference can terminate in two ways: first, when the model reaches a threshold of confidence (entropy of hidden states, $\chi^{(i)}$) about the to-be-recognized syllable, word, or sentence. This happens when the model successfully infers a known syllable, word, or sentence.

Second, the inference can terminate when it reaches a maximum number of iterations $K_{\max}^{(i)}$ at each i -th level. This sets the maximum number of times Level 1 can jump between letters to recognize a syllable, the maximum number of times Level 2 can jump between syllables to recognize a word, or the maximum number of times Level 3 can jump between words to recognize a sentence. In our simulations, we set $K_{\max}^{(i)}$ at a high value of 15, which is almost never reached in practice.

However, in the simulations shown in Fig. 7, we set $K_{\max}^{(3)} = 7$ and $K_{\max}^{(2)} = K_{\max}^{(1)} = 6$. Level 1 successfully infers all the syllables within 3 iterations and never reaches $K_{\max}^{(1)}$. However, Level 2 fails to recognize the unknown word *offbeat*: it continues jumping between the syllables *off* and *beat* until it reaches the maximum number of allowed iterations (6 iterations, indicated in the grey panel). The inference of the current word is halted, and a low confidence message is reported to the level above, after which Level 2 continues with the next words that it successfully recognizes. Similarly, Level 3 fails to infer the unknown sentence after the maximum number of iterations (7 iterations) despite correctly recognizing most of the words. At the end of the simulation, the model identifies that the cause of failure is at Level 2, as Level 1 correctly recognized all the syllables. Consequently, the model reads the unknown word syllable-by-syllable, corresponding to the nonlexical route in dual route theories of reading [8].

Data and Software Availability

Code, utilities and datasets used for the development of the computational model, simulations and data analyses are openly available at the GitHub repository: https://github.com/donnarumma/HAI_LANGUAGE.

Acknowledgments

This research received funding from the European Union’s Horizon 2020 Framework Programme for Research and Innovation under the Specific Grant Agreements No. 945539 (Human Brain Project SGA3) and No. 952215 (TAILOR) to GP; the European Research Council under the Grant Agreement No. 820213 (ThinkAhead) to GP; the PNRR MUR projects PE0000013-FAIR and IR0000011-EBRAINS-Italy to GP; the MUR PRIN2020 project “Free energy principle and the brain: neuronal and phylogenetic mechanisms of

Bayesian inference” - Grant N. 2020529PCP to FD. The funders had no role in study design, data collection and analysis, decision to publish, or preparation of the manuscript.

References

- [1] Christopher Baldassano, Janice Chen, Asieh Zadbood, Jonathan W Pillow, Uri Hasson, and Kenneth A Norman. Discovering event structure in continuous narrative perception and memory. *Neuron*, 95(3):709–721, 2017.
- [2] Christopher M Bishop and Nasser M Nasrabadi. *Pattern recognition and machine learning*. Springer, 2006.
- [3] Maria Pia Bucci, Dominique Brémond-Gignac, and Zoï Kapoula. Poor binocular coordination of saccades in dyslexic children. *Graefe’s archive for clinical and experimental ophthalmology*, 246:417–428, 2008.
- [4] Reese Butterfuss and Panayiota Kendeou. The role of executive functions in reading comprehension. *Educational Psychology Review*, 30:801–826, 2018.
- [5] Cheryl M Capek, Daphne Bavelier, David Corina, Aaron J Newman, Peter Jezzard, and Helen J Neville. The cortical organization of audio-visual sentence comprehension: an fmri study at 4 tesla. *Cognitive brain research*, 20(2):111–119, 2004.
- [6] Charlotte Caucheteux, Alexandre Gramfort, and Jean-Rémi King. Evidence of a predictive coding hierarchy in the human brain listening to speech. *Nature human behaviour*, 7(3):430–441, 2023.
- [7] Claire HC Chang, Samuel A Nastase, and Uri Hasson. Information flow across the cortical timescale hierarchy during narrative construction. *Proceedings of the National Academy of Sciences*, 119(51):e2209307119, 2022.
- [8] Max Coltheart. Modeling reading: The dual-route approach. *The science of reading: A handbook*, 1:6–23, 2005.
- [9] Maria De Luca, Enrico Di Pace, Anna Judica, Donatella Spinelli, and Pierluigi Zoccolotti. Eye movement patterns in linguistic and non-linguistic tasks in developmental surface dyslexia. *Neuropsychologia*, 37(12):1407–1420, 1999.
- [10] Jacob Devlin, Ming-Wei Chang, Kenton Lee, and Kristina Toutanova. Bert: Pre-training of deep bidirectional transformers for language understanding. *NAACL HLT 2019 - 2019 Conference of the North American Chapter of the Association for Computational Linguistics: Human Language Technologies - Proceedings of the Conference*, 1:4171 – 4186, 2019. Cited by: 22093.
- [11] Francesco Donnarumma, Marcello Costantini, Ettore Ambrosini, Karl Friston, and Giovanni Pezzulo. Action perception as hypothesis testing. *Cortex*, 89:45–60, 2017.
- [12] Marcello Ferro, Dimitri Ognibene, Giovanni Pezzulo, and Vito Pirrelli. Reading as active sensing: a computational model of gaze planning during word recognition. *Frontiers in Neurorobotics*, 4:6, 2010.
- [13] Stefan L Frank, Leun J Otten, Giulia Galli, and Gabriella Vigliocco. The erp response to the amount of information conveyed by words in sentences. *Brain and language*, 140:1–11, 2015.
- [14] Leon Franzen, Zoey Stark, and Aaron P Johnson. Individuals with dyslexia use a different visual sampling strategy to read text. *Scientific reports*, 11(1):6449, 2021.
- [15] Karl Friston. A theory of cortical responses. *Philosophical transactions of the Royal Society B: Biological sciences*, 360(1456):815–836, 2005.

- [16] Karl Friston. The free-energy principle: a unified brain theory? *Nature reviews neuroscience*, 11(2):127–138, 2010.
- [17] Karl Friston, Rick A Adams, Laurent Perrinet, and Michael Breakspear. Perceptions as hypotheses: saccades as experiments. *Frontiers in psychology*, 3:151, 2012.
- [18] Karl Friston, Thomas FitzGerald, Francesco Rigoli, Philipp Schwartenbeck, and Giovanni Pezzulo. Active inference: a process theory. *Neural computation*, 29(1):1–49, 2017.
- [19] Karl J Friston, Noor Sajid, David Ricardo Quiroga-Martinez, Thomas Parr, Cathy J Price, and Emma Holmes. Active listening. *Hearing research*, 399:107998, 2021.
- [20] Ariel Goldstein, Zaid Zada, Eliav Buchnik, Mariano Schain, Amy Price, Bobbi Aubrey, Samuel A Nastase, Amir Feder, Dotan Emanuel, Alon Cohen, et al. Shared computational principles for language processing in humans and deep language models. *Nature neuroscience*, 25(3):369–380, 2022.
- [21] Riitta Hari, Hanna Renvall, and Topi Tanskanen. Left minineglect in dyslexic adults. *Brain*, 124(7):1373–1380, 2001.
- [22] Uri Hasson, Janice Chen, and Christopher J Honey. Hierarchical process memory: memory as an integral component of information processing. *Trends in cognitive sciences*, 19(6):304–313, 2015.
- [23] Stefan Hawelka, Benjamin Gagl, and Heinz Wimmer. A dual-route perspective on eye movements of dyslexic readers. *Cognition*, 115(3):367–379, 2010.
- [24] Micha Heilbron, Kristijan Armeni, Jan-Mathijs Schoffelen, Peter Hagoort, and Floris P De Lange. A hierarchy of linguistic predictions during natural language comprehension. *Proceedings of the National Academy of Sciences*, 119(32):e2201968119, 2022.
- [25] Tzipi Horowitz-Kraus, Nicole Cicchino, Merav Amiel, Scott K Holland, and Zvia Breznitz. Reading improvement in english-and hebrew-speaking children with reading difficulties after reading acceleration training. *Annals of dyslexia*, 64:183–201, 2014.
- [26] Florian Hutzler and Heinz Wimmer. Eye movements of dyslexic children when reading in a regular orthography. *Brain and language*, 89(1):235–242, 2004.
- [27] Takuya Isomura, Kiyoshi Kotani, Yasuhiko Jimbo, and Karl Friston. Experimental validation of the free-energy principle with in vitro neural networks. *bioRxiv*, pages 2022–10, 2022.
- [28] Sagi Jaffe-Dax, Ofri Raviv, Nori Jacoby, Yonatan Loewenstein, and Merav Ahissar. A computational model of implicit memory captures dyslexics’ perceptual deficits. *Journal of Neuroscience*, 35(35):12116–12126, 2015.
- [29] Stephanie Jainta and Zoï Kapoula. Dyslexic children are confronted with unstable binocular fixation while reading. *PloS one*, 6(4):e18694, 2011.
- [30] Miika Koskinen, Mikko Kurimo, Joachim Gross, Aapo Hyvärinen, and Riitta Hari. Brain activity reflects the predictability of word sequences in listened continuous speech. *Neuroimage*, 219:116936, 2020.
- [31] Marta Kutas and Steven A Hillyard. Brain potentials during reading reflect word expectancy and semantic association. *Nature*, 307(5947):161–163, 1984.
- [32] G Reid Lyon, Sally E Shaywitz, and Bennett A Shaywitz. A definition of dyslexia. *Annals of dyslexia*, 53:1–14, 2003.

- [33] Manfred MacKeben, Susanne Trauzettel-Klosinski, Jens Reinhard, Ute Dürrwächter, Martin Adler, and Gunther Klosinski. Eye movement control during single-word reading in dyslexics. *Journal of Vision*, 4(5):4–4, 2004.
- [34] José M Maisog, Erin R Einbinder, D Lynn Flowers, Peter E Turkeltaub, and Guinevere F Eden. A meta-analysis of functional neuroimaging studies of dyslexia. *Annals of the new York Academy of Sciences*, 1145(1):237–259, 2008.
- [35] Christopher D Manning, Kevin Clark, John Hewitt, Urvashi Khandelwal, and Omer Levy. Emergent linguistic structure in artificial neural networks trained by self-supervision. *Proceedings of the National Academy of Sciences*, 117(48):30046–30054, 2020.
- [36] Dennis Norris. The bayesian reader: explaining word recognition as an optimal bayesian decision process. *Psychological review*, 113(2):327, 2006.
- [37] Beth A O’Brien, J Stephen Mansfield, and Gordon E Legge. The effect of print size on reading speed in dyslexia. *Journal of Research in Reading*, 28(3):332–349, 2005.
- [38] Giorgio Parisi. *Statistical field theory*. Frontiers in physics. Addison-Wesley, Redwood City, CA, 1988.
- [39] Thomas Parr, Giovanni Pezzulo, and Karl J Friston. *Active inference: the free energy principle in mind, brain, and behavior*. MIT Press, 2022.
- [40] Conrad Perry, Marco Zorzi, and Johannes C Ziegler. Understanding dyslexia through personalized large-scale computational models. *Psychological science*, 30(3):386–395, 2019.
- [41] Chloé Prado, Matthieu Dubois, and Sylviane Valdois. The eye movements of dyslexic children during reading and visual search: impact of the visual attention span. *Vision research*, 47(19):2521–2530, 2007.
- [42] Cathy J Price. A review and synthesis of the first 20 years of pet and fmri studies of heard speech, spoken language and reading. *Neuroimage*, 62(2):816–847, 2012.
- [43] Friedemann Pulvermüller. Words in the brain’s language. *Behavioral and brain sciences*, 22(2):253–279, 1999.
- [44] Alec Radford, Jeffrey Wu, Rewon Child, David Luan, Dario Amodei, Ilya Sutskever, et al. Language models are unsupervised multitask learners. *OpenAI blog*, 1(8):9, 2019.
- [45] Franck Ramus. Developmental dyslexia: specific phonological deficit or general sensorimotor dysfunction? *Current opinion in neurobiology*, 13(2):212–218, 2003.
- [46] Rajesh PN Rao and Dana H Ballard. Predictive coding in the visual cortex: a functional interpretation of some extra-classical receptive-field effects. *Nature neuroscience*, 2(1):79–87, 1999.
- [47] Keith Rayner. Eye movements, perceptual span, and reading disability. *Annals of Dyslexia*, pages 163–173, 1983.
- [48] Lea-Maria Schmitt, Julia Erb, Sarah Tune, Anna U Rysop, Gesa Hartwigsen, and Jonas Obleser. Predicting speech from a cortical hierarchy of event-based time scales. *Science Advances*, 7(49):eabi6070, 2021.
- [49] John Stein and Vincent Walsh. To see but not to read; the magnocellular theory of dyslexia. *Trends in neurosciences*, 20(4):147–152, 1997.
- [50] Paula Tallal. Improving language and literacy is a matter of time. *Nature Reviews Neuroscience*, 5(9):721–728, 2004.

- [51] Hugo Weissbart, Katerina D Kandylaki, and Tobias Reichenbach. Cortical tracking of surprisal during continuous speech comprehension. *Journal of cognitive neuroscience*, 32(1):155–166, 2020.
- [52] Roel M Willems, Stefan L Frank, Annabel D Nijhof, Peter Hagoort, and Antal Van den Bosch. Prediction during natural language comprehension. *Cerebral Cortex*, 26(6):2506–2516, 2016.
- [53] Asieh Zadbood, Janice Chen, Yuan Chang Leong, Kenneth A Norman, and Uri Hasson. How we transmit memories to other brains: constructing shared neural representations via communication. *Cerebral cortex*, 27(10):4988–5000, 2017.
- [54] Pierluigi Zoccolotti, Maria De Luca, Enrico Di Pace, Filippo Gasperini, Anna Judica, and Donatella Spinelli. Word length effect in early reading and in developmental dyslexia. *Brain and language*, 93(3):369–373, 2005.
- [55] Marco Zorzi, Chiara Barbiero, Andrea Facoetti, Isabella Lonciari, Marco Carrozzi, Marcella Montico, Laura Bravar, Florence George, Catherine Pech-Georgel, and Johannes C Ziegler. Extra-large letter spacing improves reading in dyslexia. *Proceedings of the National Academy of Sciences*, 109(28):11455–11459, 2012.

A Supplementary Information

In this section, we provide the tables of statistics from the simulations presented in the main article (found in Supplementary Tables section) and the Datasets of sentences and words used in the simulation (found in Datasets section).

Supplementary tables

Below are the supplementary tables presenting statistics related to the simulations discussed in the main manuscript.

Supplementary tables for Simulation 1

Table S.1 displays the accuracy and probability assigned to the correct words. Table S.2 shows the T-tests on total saccades and backward saccades. Table S.3 presents the T-tests for the amplitude of forward and backward saccades. The p -values lower to 0.05 are indicated in bold.

Table S.1: Simulation 1: Reading words of 4 or 8 letters. The table presents the accuracy and the probability assigned to the correct words by 4 different models: the *Control model* (CM), the *Dyslexic model* (DM) variant with noise at Level 1 only, the *Dyslexic model* (DM) variant with noise at Level 2 only, and the *Dyslexic model* (DM) with noise at both levels. See Fig. 2 and the main text for details.

| | 4 - LETTER | | 8 - LETTER | |
|----------------------|------------|--------------------------------|------------|--------------------------------|
| | ACCURACY | PROBABILITY | ACCURACY | PROBABILITY |
| CONTROL MODEL | 100 | $1.00 \pm 1.03 \cdot 10^{-14}$ | 100 | $1.00 \pm 7.85 \cdot 10^{-15}$ |
| DM -NOISE ON LEVEL 1 | 100 | $1.00 \pm 3.32 \cdot 10^{-04}$ | 100 | $0.99 \pm 3.82 \cdot 10^{-04}$ |
| DM -NOISE ON LEVEL 2 | 99 | $0.99 \pm 3.73 \cdot 10^{-15}$ | 97 | $0.97 \pm 1.38 \cdot 10^{-02}$ |
| DYSLEXIC MODEL | 99 | $0.99 \pm 3.32 \cdot 10^{-04}$ | 97 | $0.97 \pm 1.15 \cdot 10^{-02}$ |

Supplementary tables for Simulation 2

Table S.4 display the accuracy and probability assigned to the correct words. Table S.5 shows the T-tests on total saccades and back saccades. Table S.6 presents the T-tests for amplitude of forward and backward saccades. The p -values lower to 0.05 are indicated in bold.

Simulation 4

Table S.7 presents T-tests on total number of saccades and the number backward saccades when the model is augmented with the topic of the sentence at Level 3 of the hierarchy. The p -values lower to 0.05 are indicated in bold.

Table S.2: Simulation 1. T-tests for simulation of 4-letter and 8-letter word reading. The table displays the results of T-tests conducted on the total number of saccades and the number of backward saccades for different models with respect to the *Control model* (CM): the *Dyslexic model* (DM) variant with noise at Level 1 (syllable) only, the *Dyslexic model* (DM) variant with noise at Level 2 (word) only, and the *Dyslexic model* (DM) with noise at both levels. See Fig. 3 and the main text for details.

| | TOTAL NUMBER OF SACCADES | | NUMBER OF BACKWARD SACCADES | |
|--------------------|---|---|---|---|
| | 4 - LETTER | 8 - LETTER | 4 - LETTER | 8 - LETTER |
| DM - NOISE LEVEL 1 | $F[1, 198] = 17.6, p \approx \mathbf{4.1 \cdot 10^{-05}}$ | $F[1, 198] = 12.7, p \approx \mathbf{4.5 \cdot 10^{-04}}$ | $F[1, 198] = 21.5, p \approx \mathbf{6.5 \cdot 10^{-06}}$ | $F[1, 198] = 17.5, p \approx \mathbf{4.4 \cdot 10^{-05}}$ |
| DM - NOISE LEVEL 2 | $F[1, 196] = 4.4, p \approx \mathbf{3.6 \cdot 10^{-02}}$ | $F[1, 190] = 5.2, p \approx \mathbf{2.4 \cdot 10^{-02}}$ | $F[1, 198] = 4.8, p \approx \mathbf{3.0 \cdot 10^{-02}}$ | $F[1, 190] = 5.7, p \approx \mathbf{1.8 \cdot 10^{-02}}$ |
| DYSLEXIC MODEL | $F[1, 196] = 16.7, p \approx \mathbf{6.4 \cdot 10^{-05}}$ | $F[1, 192] = 10.7, p \approx \mathbf{1.3 \cdot 10^{-03}}$ | $F[1, 196] = 21.7, p \approx \mathbf{5.8 \cdot 10^{-06}}$ | $F[1, 192] = 13.3, p \approx \mathbf{3.4 \cdot 10^{-04}}$ |

Table S.3: Simulation 1. T-tests for simulation of 4-letter and 8-letter word reading. The table displays the results of T-tests conducted on the amplitude of forward and backward saccades for different models with respect to the *Control model* (CM): the *Dyslexic model* (DM) variant with noise at Level 1 (syllable) only, the *Dyslexic model* (DM) variant with noise at Level 2 (word) only, and the *Dyslexic model* (DM) with noise at both levels. See Fig. 4 and the main text for details.

| | AMPLITUDE OF FORWARD SACCADDES | | AMPLITUDE OF BACKWARD SACCADDES | |
|----------------|---|--|---|--|
| | 4 - LETTER | 8 - LETTER | 4 - LETTER | 8 - LETTER |
| DYSLEXIC MODEL | $F[1, 844] = 9.4, p \approx 2.2 \cdot 10^{-03}$ | $F[1, 678] = 46.5, p \approx 2.0 \cdot 10^{-11}$ | $F[1, 321] = 133.5, p \approx 4.6 \cdot 10^{-26}$ | $F[1, 312] = 24.5, p \approx 1.2 \cdot 10^{-06}$ |

Table S.4: Simulation 2: Reading sentences of 4 or 8 words. The table presents the accuracy and the probability assigned to the correct words by 4 different models: the *Control model* (CM), the *Dyslexic model* (DM) variant with noise at Level 1 only, the *Dyslexic model* (DM) variant with noise at Level 2 only, the *Dyslexic model* (DM) variant with noise at Level 3 only, and the *Dyslexic model* (DM) with noise at all levels. See Fig. 2 and the main text for details.

| | 4 - WORD | | 8 - WORD | |
|-----------------------|----------|--------------------------------|----------|--------------------------------|
| | ACCURACY | PROBABILITY | ACCURACY | PROBABILITY |
| CONTROL MODEL | 100 | $1.00 \pm 3.66 \cdot 10^{-16}$ | 100 | $1.00 \pm 3.21 \cdot 10^{-12}$ |
| DM - NOISE ON LEVEL 1 | 100 | $1.00 \pm 3.64 \cdot 10^{-06}$ | 100 | $1.00 \pm 5.69 \cdot 10^{-08}$ |
| DM - NOISE ON LEVEL 2 | 100 | $1.00 \pm 3.40 \cdot 10^{-07}$ | 100 | $1.00 \pm 3.21 \cdot 10^{-12}$ |
| DM - NOISE ON LEVEL 3 | 97 | $0.97 \pm 4.25 \cdot 10^{-03}$ | 93 | $0.93 \pm 1.04 \cdot 10^{-02}$ |
| DYSLEXIC MODEL | 96 | $0.96 \pm 4.41 \cdot 10^{-03}$ | 93 | $0.93 \pm 1.04 \cdot 10^{-02}$ |

Table S.5: Simulation 2. T-tests for simulation of 4-word and 8-word sentence reading. The table displays the results of T-tests conducted on the total number of saccades and the number of backward saccades for different models with respect to the *Control model* (CM): the *Dyslexic model* (DM) variant with noise at Level 1 (syllable) only, the *Dyslexic model* (DM) variant with noise at Level 2 (word) only, the *Dyslexic model* (DM) variant with noise at Level 3 (sentence) only, and the *Dyslexic model* (DM) with noise at all levels. See Fig. 5 and the main text for details.

| | TOTAL NUMBER OF SACCADDES | | NUMBER OF BACKWARD SACCADDES | |
|--------------------|--|---|--|---|
| | 4 - WORD | 8 - WORD | 4 - WORD | 8 - WORD |
| DM - NOISE LEVEL 1 | $F[1, 198] = 0.02, p \approx 0.90$ | $F[1, 198] = 0.01, p \approx 0.92$ | $F[1, 198] = 0.41, p \approx 0.52$ | $F[1, 198] = 0.82, p \approx 0.37$ |
| DM - NOISE LEVEL 2 | $F[1, 198] = 0.97, p \approx 0.33$ | $F[1, 198] = 0.31, p \approx 0.58$ | $F[1, 198] = 0.01, p \approx 0.90$ | $F[1, 198] = 1.86, p \approx 0.17$ |
| DM - NOISE LEVEL 3 | $F[1, 198] = 66.8, p \approx 3.5 \cdot 10^{-14}$ | $F[1, 196] = 105.9, p \approx 3.9 \cdot 10^{-20}$ | $F[1, 198] = 44.7, p \approx 2.3 \cdot 10^{-10}$ | $F[1, 196] = 119.4, p \approx 5.1 \cdot 10^{-22}$ |
| DYSLEXIC MODEL | $F[1, 198] = 75.5, p \approx 1.4 \cdot 10^{-15}$ | $F[1, 196] = 113.6, p \approx 3.2 \cdot 10^{-21}$ | $F[1, 198] = 53.2, p \approx 7.1 \cdot 10^{-12}$ | $F[1, 196] = 117.7, p \approx 8.8 \cdot 10^{-22}$ |

Table S.6: Simulation 2. T-tests for simulation of 4-word and 8-word sentence reading. The table displays the results of T-tests conducted on the amplitude of forward and backward saccades for different models with respect to the *Control model* (CM): the *Dyslexic model* (DM) variant with noise at Level 1 (syllable) only, the *Dyslexic model* (DM) variant with noise at Level 2 (word) only, the *Dyslexic model* (DM) variant with noise at Level 3 (sentence) only, and the *Dyslexic model* (DM) with noise at all levels. See Fig. 6 and the main text for details.

| | AMPLITUDE OF FORWARD SACCADDES | | AMPLITUDE OF BACKWARD SACCADDES | |
|----------------|--|---|--|--|
| | 4 - WORD | 8 - WORD | 4 - WORD | 8 - WORD |
| DYSLEXIC MODEL | $F[1, 878] = 18.0, p \approx 2.5 \cdot 10^{-05}$ | $F[1, 1238] = 10.9, p \approx 9.8 \cdot 10^{-04}$ | $F[1, 318] = 14.7, p \approx 1.5 \cdot 10^{-04}$ | $F[1, 350] = 42.5, p \approx 2.5 \cdot 10^{-10}$ |

Table S.7: Simulation 4. T-tests for simulation of a 9-word sentence reading, belonging to different topics. The table displays the results of T-tests conducted on the total number of saccades and the number of backward saccades for different models with respect to the *Control model* (CM): the *Dyslexic model* (DM) variant with noise at Level 1 (syllable) only, the *Dyslexic model* (DM) variant with noise at Level 2 (word) only, the *Dyslexic model* (DM) variant with noise at Level 3 (sentence) only, and the *Dyslexic model* (DM) with noise at all levels. See Fig. 8 and the main text for details.

| | TOTAL NUMBER OF SACCADDES | NUMBER OF BACKWARD SACCADDES |
|-----------------------------------|--|------------------------------------|
| FLAT PRIORS VS INFORMATIVE PRIORS | $F[1, 198] = 4.07, p \approx 4.1 \cdot 10^{-03}$ | $F[1, 198] = 2.57, p \approx 0.11$ |

Table S.8: This table reports the mean number of characters, the standard deviation, minimum and maximum number of characters that compose the relative set of sentences used in the simulations.

| | MEAN | STANDARD DEVIATION | MIN | MAX |
|-------------------------|-------|-----------------------|-----|-----|
| SIMULATION 2 (4 - WORD) | 25.96 | 1.96 | 21 | 31 |
| SIMULATION 2 (8 - WORD) | 50.24 | 1.64 | 47 | 55 |
| SIMULATION 4 | 69.55 | 5.02 | 61 | 82 |

Datasets

In this section, we present the datasets utilized in our simulations. Information regarding content length in the datasets can be found in Table S.8. Furthermore, Table S.9 displays the dictionary of words used in Simulation 1, while Table S.10 provides insight into the sentences used in Simulation 2. Additionally, Simulation 4’s sentences and corresponding labels are showcased in Table S.11.

Table S.9: Dictionary used in Simulation 1 (words extracted from the BERT Dictionary)

| 1 - LETTER | 2- LETTER | 3- LETTER | 4- LETTER | 5- LETTER | 6- LETTER | 7- LETTER | 8- LETTER |
|------------|-----------|-----------|-----------|-----------|-----------|-----------|-----------|
| A | AC | AMC | ARES | AGREE | ACTING | AIRPORT | ACQUIRED |
| B | AL | ARM | ARTS | ANZAC | ADVENT | ALCOHOL | ACTUALLY |
| C | AM | ATA | ASKS | ARDEN | AIRMEN | ANGRILY | ADVANCED |
| D | AR | AUS | BEDS | ARIEL | ANGLIA | ARCADIA | ALPHABET |
| E | AW | BAO | BORE | AZURE | ARMAND | ASSURED | AMERICAN |
| F | AX | BEG | BRET | BARED | AUSTEN | AVENUES | APPLETON |
| G | BF | BEN | BUSY | BEGUN | BECKER | BALANCE | ARGUMENT |
| H | BI | BIT | BUTT | BIRDS | BEIRUT | BENGALS | ARRANGED |
| I | BK | BOP | CALE | BLAND | BERMAN | BERWICK | ATLANTIC |
| J | BO | BUY | CARL | BUICK | BIGGER | BOUNCED | BALANCED |
| K | BR | CAB | COAL | BULGE | BISHOP | BURUNDI | BASILICA |
| L | BT | CAD | COLA | BUTCH | BUMPER | CAREERS | BENEDICT |
| M | CA | CAI | COOL | CELLO | BURDEN | CEILING | BOTSWANA |
| N | CB | CEO | CUBS | CLEAR | CANTOR | CHANCEL | BOULDERS |
| O | CH | COE | DIRT | CLUBS | CAUSAL | CLICKED | BREACHED |
| P | CL | CPU | DOIN | CODES | CEREAL | CLIENTS | BREAKING |
| Q | CM | DEX | DOVE | COSTS | CESARE | COMMITTS | CADILLAC |
| R | CN | DIG | DRIP | CRIED | CESSNA | CROOKED | CAMPBELL |
| S | CO | DIP | DRUM | CURLY | CHICKS | DERRICK | CARRYING |
| T | CP | EKI | ELLE | DANNY | CLOCKS | DESCENT | CATALINA |
| U | CU | EPA | EMIR | DATED | COINED | DESPAIR | COLISEUM |
| V | ED | ETA | EMMA | DEBUT | DECKER | DEvised | COLUMBIA |
| W | EH | FIG | FANS | DISCS | DISMAY | EDUARDO | CONNECTS |
| X | EL | FLU | FEES | DOUBT | DRINKS | EMBASSY | CONVINCE |
| Y | EM | FUN | FIJI | DUCKS | EXEMPT | EMERSON | CUMMINGS |
| Z | EU | HAN | FINS | DUMMY | FACADE | EMPLOYES | CURRENCY |
| | FI | HBO | FLOP | ECOLE | FINLEY | ENEMIES | CYCLONES |
| | FL | HEM | FLUX | ELIZA | GENTRY | ESCAPES | CYLINDER |
| | FT | HIT | FRAN | ESSEN | HAILEY | EXHAUST | DARKENED |
| | FU | HOP | GIFT | FEMME | HANNAH | FAINTLY | DECEASED |
| | FX | HUE | GIGS | FISTS | HASSAN | FLEDGED | DECIDING |
| | GE | IBN | GLOW | FLOOR | HATRED | FORSTER | DISABLED |
| | GI | ICE | GRAM | FLOYD | HELMUT | FREEWAY | DISASTER |
| | GO | ICH | GREY | GOUGH | HOOVER | FRONTED | DONNELLY |
| | GS | ICT | HAAS | GROWS | HUTTON | GALILEO | EMERITUS |
| | GT | ILE | HANK | GRUNT | HYBRID | GEOLOGY | EMPLOYER |
| | GU | ION | HILL | GUARD | INCOME | GLIDING | EPILOGUE |
| | HA | IRA | HISS | HELLO | INPUTS | HAMBURG | EREBIDAE |
| | HC | KIM | HUEY | HIRES | INTERN | HANDLED | EVACUATE |
| | HM | LAL | INDY | HORDE | JOSEPH | HIGHEST | EVOLVING |
| | HO | LAY | JACE | JOINT | JUAREZ | HONNEUR | EXAMINER |
| | HU | LEG | JAIN | JOYCE | KHYBER | HORNETS | FABULOUS |
| | IK | LES | JEAN | LATER | LANDON | HOWEVER | FIGHTERS |
| | IN | LOU | JING | LEANS | LENGTH | HOWLING | FRANKLIN |
| | IO | LTD | KRIS | LEAVE | LENNON | HUNCHEd | FRICTION |
| | IR | MED | LAMA | LOOSE | LIKELY | INHALED | GESTURES |
| | IX | MPH | LANG | LOVER | LILITH | IRANIAN | GROUPING |
| | JA | MPS | LETO | LUCHA | LITTER | JEALOUS | HOMICIDE |
| | JD | MSC | LIAR | LYDIA | MADRAS | JUSTINE | IMPERIAL |
| | KE | MUD | MACK | MAHAL | MANUEL | KNIGHTS | INCURRED |
| | KG | NBA | MARS | MERGE | MARGIN | LABELED | INITIATE |
| | KN | NHL | MASK | MINSK | MARKED | LASTING | INJURIES |
| | KO | NHS | MEAT | MISSY | MCLEAN | LEBANON | INSANITY |
| | KS | NIK | MIKA | MIXED | MOLINA | MANNING | JUDICIAL |
| | LC | NOS | MOJO | MOMMA | MUSEUM | MCBRIDE | LABRADOR |
| | LI | NOV | MOOD | NAILS | MYSELF | MORALLY | MAGAZINE |
| | LP | NPR | MUCH | NORMA | NEWELL | MUSCLED | MARATHON |
| | MG | NYC | NEAT | OLDER | ONIONS | NATALIE | MEANINGS |
| | MI | OFF | NINO | OUTTA | OPENLY | NEURONS | MOHAMMAD |
| | ML | OUT | NOSE | PAPUA | OPPOSE | NEVILLE | MONSIEUR |
| | MR | PAT | NRHP | PATIO | PANZER | NIKOLAI | MOROCCAN |
| | NA | PAU | OBOE | PIANO | PAVING | NILSSON | MOUNTING |
| | NH | PBA | OWLS | PILES | PAYTON | NOMINAL | MUSHROOM |
| | NI | PBS | PASS | PLUTO | PETALS | OFFENSE | OLYMPIAD |
| | NO | PCS | PERU | PROSE | PILOTS | ONSTAGE | PACKAGES |
| | NS | PEI | PORN | QAEDA | PLANES | PATCHES | PATERSON |
| | NT | PEW | RAAF | RALLY | POLITE | PEPTIDE | PHILLIPS |
| | NZ | PHI | RAMP | REEFS | POTION | PERFECT | POPULACE |
| | OG | PHP | RAMS | REVUE | PRAGUE | PEUGEOT | POUNDING |
| | OH | POD | RUDD | ROACH | PRICED | PIONEER | PREACHER |
| | OL | PUN | SANK | ROUEN | PULSES | PLANNED | PRESTIGE |
| | OP | ROE | SAXE | RUSSO | PUPILS | PLAYFUL | QUARTERS |
| | OS | ROM | SITU | SCOTT | RASHID | PORTICO | RAILROAD |
| | OZ | RUM | SIZE | SHORE | REPORT | PROTEST | RECEIVES |
| | PH | RYE | SLID | SINGH | RIPLEY | RAPIDLY | REJOINED |
| | PO | SAO | SODA | SITED | ROBERT | READERS | SCENARIO |
| | PR | SEA | SOON | SLAMS | RUNNER | RECITAL | SEMINOLE |
| | RC | SHI | STAY | SPRAY | SAILOR | REDWOOD | SHOOTOUT |
| | RR | SHU | STYX | SQUAT | SAXONY | REISSUE | SHOWERED |
| | RY | SPP | SUFI | STADE | SCARES | ROOSTER | SINGULAR |
| | SE | SSR | SWAM | STAFF | SCREAM | RUINING | SOMERSET |
| | SF | SUE | TEAM | STALL | SEIZED | SECURED | SOUTHEND |
| | SM | TAI | THRU | STATE | SESAME | SILENCE | SPECIALS |
| | SQ | TEA | TODD | STERN | SEVERN | SMASHED | SPEEDING |
| | SR | TEX | TOLD | STORM | SIGNAL | SPELLED | STRANDED |
| | TC | TIS | TOPS | STUMP | SPEAKS | STATION | STRIPPED |
| | TU | TNA | TRIP | TOUGH | SPINES | STEWART | SYMBOLIC |
| | TV | UFO | TUNA | TRANS | STALLS | STRANGE | TARGETED |
| | TX | VAR | UGLY | TREAT | STARTS | STRIKES | TAXATION |
| | UP | VII | USER | TREES | SURFER | SWELLED | THROTTLE |
| | UR | WAT | VEGA | VAULT | TORINO | TIGHTLY | TIMELINE |
| | VA | WAY | VIDA | VIJAY | TREVOR | TOPICAL | TOURISTS |
| | VE | WOW | VISA | VISAS | TURTLE | TURTLES | UNCOMMON |
| | VP | XII | WEEP | VOMIT | VENDOR | ULYSSES | VALENTIN |
| | VU | XVI | WHOA | WEARS | VERBAL | UNITING | VIGOROUS |
| | WC | YES | WIFE | WHORE | WANTED | UNNAMED | VILLAINS |
| | XI | YET | WINS | WRAPS | WASHED | VACANCY | WARRIORS |
| | YA | YOO | WITS | WRIST | WIRING | VISIBLE | WEREWOLF |
| | YE | ZEE | YUKI | YEMEN | WORTHY | WALKING | WORRYING |
| | YO | ZEV | ZOOM | YOUTH | XAVIER | WARTIME | ZIMBABWE |

Table S.10: Dictionary used in Simulation 2

| 4 - Word | 8 - Word |
|-------------------------------------|--|
| FAITH CONQUERS ALL OBSTACLES | FAITH CONQUERS ALL OBSTACLES AND TRASCENDS ALL ADVERSITY |
| FAITH CONQUERS EACH HURDLE | FAITH CONQUERS ALL OBSTACLES AND TRASCENDS ALL MISFORTUNE |
| FAITH CONQUERS EACH SETBACK | FAITH CONQUERS EACH HURDLE BUT TRASCENDS ALL MISFORTUNE |
| FAITH CONQUERS EVERY CHALLENGES | FAITH CONQUERS EACH SETBACK BUT SURMOUNTS ALL OBSTACLES |
| FAITH CONQUERS EVERY OBSTACLES | FAITH CONQUERS EVERY OBSTACLES AND PREVAILS OVER ADVERSITY |
| FAITH DEFEATS ALL OBSTACLES | FAITH CONQUERS EVERY OBSTACLES AND SURMOUNTS ALL OBSTACLES |
| FAITH OVERCOMES ALL HINDRANCES | FAITH DEFEATS ALL OBSTACLES AND TRASCENDS ALL ADVERSITY |
| FAITH OVERCOMES ALL OBSTACLES | FAITH DEFEATS ALL OBSTACLES AND TRASCENDS ALL MISFORTUNE |
| FAITH OVERPOWERS ALL LIMITATIONS | FAITH OVERCOMES ALL HINDRANCES AND TRASCENDS OVER MISFORTUNE |
| FAITH PREVAILS AGAINST BARRIERS | FAITH OVERCOMES ALL OBSTACLES AND TRASCENDS ALL ADVERSITY |
| FAITH PREVAILS AGAINST OBSTACLES | FAITH OVERCOMES ALL OBSTACLES AND TRASCENDS ALL MISFORTUNE |
| FAITH PREVAILS OVER EVERY ADVERSITY | FAITH OVERPOWERS ALL LIMITATIONS BUT TRASCENDS ALL MISFORTUNE |
| FAITH PREVAILS OVER OBSTACLES | FAITH PREVAILS AGAINST BARRIERS AND TRASCENDS OVER MISFORTUNE |
| FAITH SURMOUNTS ALL OBSTACLES | FAITH PREVAILS AGAINST OBSTACLES AND TRASCENDS ALL MISFORTUNE |
| FAITH SURPASSES ALL OBSTACLES | FAITH PREVAILS EVERY ADVERSITY BUT SURMOUNTS ALL OBSTACLES |
| FAITH SURPASSES ALL OPPOSITION | FAITH PREVAILS OVER ADVERSITY BUT SURMOUNTS ALL OBSTACLES |
| FAITH TRIUMPHS AGAINST OBSTACLES | FAITH PREVAILS OVER OBSTACLES AND TRASCENDS ALL MISFORTUNE |
| FAITH TRIUMPHS OVER CHALLENGES | FAITH SURMOUNTS ALL OBSTACLES AND SURMOUNTS ALL MISFORTUNE |
| FAITH TRIUMPHS OVER OBSTACLES | FAITH SURPASSES ALL OBSTACLES AND TRASCENDS ALL ADVERSITY |
| FAITH VANQUISHES ALL OBSTACLES | FAITH SURPASSES ALL OBSTACLES AND TRASCENDS ALL MISFORTUNE |
| FAITH VANQUISHES EVERY DIFFICULTY | FAITH SURPASSES ALL OBSTACLES BUT SURMOUNTS ALL ADVERSITY |
| HOPE CONQUERS ALL LIMITATIONS | FAITH SURPASSES ALL OPPOSITION BUT SURMOUNTS ALL MISFORTUNE |
| HOPE CONQUERS ALL OBSTACLES | FAITH TRIUMPHS AGAINST OBSTACLES AND TRASCENDS ALL MISFORTUNE |
| HOPE CONQUERS EACH CHALLENGES | FAITH TRIUMPHS OVER CHALLENGES AND TRASCENDS OVER MISFORTUNE |
| HOPE CONQUERS EACH HINDRANCES | FAITH TRIUMPHS OVER OBSTACLES AND TRASCENDS ALL ADVERSITY |
| HOPE CONQUERS EACH HURDLE | FAITH TRIUMPHS OVER OBSTACLES AND TRASCENDS ALL MISFORTUNE |
| HOPE CONQUERS EACH INHIBITION | FAITH VANQUISHES ALL OBSTACLES AND TRASCENDS ALL MISFORTUNE |
| HOPE CONQUERS EACH LIMITATIONS | FAITH VANQUISHES EVERY DIFFICULTY BUT TRASCENDS ALL MISFORTUNE |
| HOPE CONQUERS EACH SETBACK | HOPE CONQUERS ALL OBSTACLES AND TRASCENDS ALL ADVERSITY |
| HOPE CONQUERS EVERY ADVERSITY | HOPE CONQUERS ALL OBSTACLES AND TRASCENDS ALL MISFORTUNE |
| HOPE CONQUERS EVERY BARRIERS | HOPE CONQUERS EACH SETBACK BUT SURMOUNTS ALL OBSTACLES |
| HOPE CONQUERS EVERY CHALLENGES | HOPE DEFEATS ALL OBSTACLES AND TRASCENDS ALL ADVERSITY |
| HOPE CONQUERS EVERY DIFFICULTY | HOPE DEFEATS ALL OBSTACLES AND TRASCENDS ALL MISFORTUNE |
| HOPE CONQUERS EVERY HURDLE | HOPE OVERCOMES ALL OBSTACLES AND TRASCENDS ALL ADVERSITY |
| HOPE CONQUERS EVERY OBSTACLES | HOPE OVERCOMES ALL OBSTACLES AND TRASCENDS ALL MISFORTUNE |
| HOPE CONQUERS EVERY RESTRAINT | HOPE PREVAILS OVER OBSTACLES AND TRASCENDS ALL ADVERSITY |
| HOPE DEFEATS ALL OPPOSITION | HOPE PREVAILS OVER OBSTACLES AND TRASCENDS ALL MISFORTUNE |
| HOPE OVERCOMES ALL CHALLENGES | HOPE SURPASSES ALL OBSTACLES AND TRASCENDS ALL ADVERSITY |
| HOPE OVERCOMES EACH BOUNDARY | HOPE SURPASSES ALL OBSTACLES AND TRASCENDS ALL MISFORTUNE |
| HOPE OVERCOMES EACH HINDRANCES | HOPE TRIUMPHS OVER OBSTACLES AND TRASCENDS ALL ADVERSITY |
| HOPE PREVAILS AGAINST ADVERSITY | HOPE TRIUMPHS OVER OBSTACLES AND TRASCENDS ALL MISFORTUNE |
| HOPE PREVAILS AGAINST BARRIERS | LOVE CONQUERS ALL ADVERSITY AND TRASCENDS ALL ADVERSITY |
| HOPE PREVAILS AGAINST IMPEDIMENT | LOVE CONQUERS ALL ADVERSITY AND TRASCENDS ALL MISFORTUNE |
| HOPE PREVAILS OVER OBSTACLES | LOVE CONQUERS ALL ADVERSITY BUT TRASCENDS ALL MISFORTUNE |
| HOPE SURMOUNTS ALL DIFFICULTIES | LOVE CONQUERS ALL ADVERSITY BUT TRASCENDS EVERY MISFORTUNE |
| HOPE SURPASSES ALL OBSTACLES | LOVE CONQUERS ALL BOUNDARIES AND TRASCENDS ALL ADVERSITY |
| HOPE SURPASSES EVERY CONFINEMENT | LOVE CONQUERS ALL BOUNDARIES AND TRASCENDS ALL MISFORTUNE |
| HOPE SURPASSES EVERY OBSTACLES | LOVE CONQUERS ALL BOUNDARIES BUT TRASCENDS ALL MISFORTUNE |
| HOPE TRASCENDS EACH RESTRICTION | LOVE CONQUERS ALL BOUNDARIES BUT TRASCENDS EVERY MISFORTUNE |
| HOPE TRIUMPHS AGAINST OBSTACLES | LOVE CONQUERS ALL DIFFERENCES AND TRASCENDS ALL ADVERSITY |
| HOPE TRIUMPHS OVER CHALLENGES | LOVE CONQUERS ALL DIFFERENCES AND TRASCENDS ALL MISFORTUNE |
| HOPE VANQUISHES ALL HINDRANCES | LOVE CONQUERS ALL DIFFERENCES BUT TRASCENDS ALL MISFORTUNE |
| LOVE OVERCOMES EACH HINDRANCES | LOVE CONQUERS ALL DIFFERENCES BUT TRASCENDS EVERY MISFORTUNE |
| LOVE CONQUERS ALL ADVERSITY | LOVE CONQUERS ALL OBSTACLES AND TRASCENDS ALL ADVERSITY |
| LOVE CONQUERS ALL BOUNDARIES | LOVE CONQUERS ALL OBSTACLES AND TRASCENDS ALL MISFORTUNE |
| LOVE CONQUERS ALL DIFFERENCES | LOVE CONQUERS ALL OBSTACLES BUT TRASCENDS ALL ADVERSITY |
| LOVE CONQUERS ALL OBSTACLES | LOVE CONQUERS ALL OBSTACLES BUT TRASCENDS EVERY ADVERSITY |
| LOVE CONQUERS ANY OBSTACLES | LOVE CONQUERS EVERY BARRIERS AND PREVAILS OVER ADVERSITY |
| LOVE CONQUERS EACH OBSTACLES | LOVE CONQUERS EVERY OBSTACLES BUT TRASCENDS ALL MISFORTUNE |
| LOVE CONQUERS EVERY BARRIERS | LOVE DEFEATS ALL OBSTACLES AND PREVAILS OVER ADVERSITY |
| LOVE CONQUERS EVERY CHALLENGES | LOVE OVERCOMES ALL OBSTACLES AND CONQUERS ALL ADVERSITY |
| LOVE CONQUERS EVERY CONFINEMENT | LOVE OVERCOMES ALL OBSTACLES AND CONQUERS ALL MISFORTUNE |
| LOVE CONQUERS EVERY DIFFICULTY | LOVE OVERCOMES ALL OBSTACLES AND CONQUERS EVERY OBSTACLES |
| LOVE CONQUERS EVERY HINDRANCES | LOVE OVERCOMES ALL OBSTACLES AND TRASCENDS ALL ADVERSITY |
| LOVE CONQUERS EVERY HURDLE | LOVE OVERCOMES ALL OBSTACLES AND TRASCENDS ALL MISFORTUNE |
| LOVE CONQUERS EVERY LIMITATIONS | LOVE OVERCOMES ALL OBSTACLES BUT CONQUERS ALL ADVERSITY |
| LOVE CONQUERS EVERY OBSTACLES | LOVE OVERCOMES ALL OBSTACLES BUT CONQUERS EVERY ADVERSITY |
| LOVE CONQUERS EVERY SETBACK | LOVE OVERCOMES ALL OBSTACLES BUT TRASCENDS ALL ADVERSITY |
| LOVE DEFEATS ALL OBSTACLES | LOVE OVERCOMES ALL OBSTACLES BUT TRASCENDS EACH ADVERSITY |
| LOVE DEFEATS ALL OPPOSITION | LOVE OVERCOMES ALL OBSTACLES BUT TRASCENDS EVERY ADVERSITY |
| LOVE OVERCOMES ALL OBSTACLES | LOVE PREVAILS AGAINST CHALLENGES AND PREVAILS OVER ADVERSITY |
| LOVE PREVAILS AGAINST CHALLENGES | LOVE PREVAILS AGAINST OBSTACLES AND OVERCOMES OVER MISFORTUNE |
| LOVE PREVAILS AGAINST OBSTACLES | LOVE PREVAILS AGAINST OBSTACLES AND PREVAILS OVER ADVERSITY |
| LOVE PREVAILS OVER OBSTACLES | LOVE PREVAILS OVER OBSTACLES AND TRASCENDS ALL MISFORTUNE |
| LOVE SURMOUNTS ALL OBSTACLES | LOVE SURMOUNTS ALL OBSTACLES BUT TRASCENDS ALL ADVERSITY |
| LOVE SURPASSES ALL OBSTACLES | LOVE SURMOUNTS ALL OBSTACLES BUT TRASCENDS ALL MISFORTUNE |
| LOVE TRIUMPHS AGAINST OBSTACLES | LOVE SURPASSES ALL OBSTACLES AND PREVAILS OVER ADVERSITY |
| LOVE TRIUMPHS OVER OBSTACLES | LOVE TRIUMPHS AGAINST OBSTACLES AND DEFEATS ALL ADVERSITY |
| LOVE VANQUISHES ALL OBSTACLES | LOVE TRIUMPHS AGAINST OBSTACLES AND DEFEATS ALL OBSTACLES |
| UNITY BREAKS THROUGH ALL BARRIERS | LOVE TRIUMPHS AGAINST OBSTACLES AND DEFEATS EACH ADVERSITY |
| UNITY CONQUERS AGAINST ODDS | LOVE TRIUMPHS AGAINST OBSTACLES AND DEFEATS OVER ADVERSITY |
| UNITY CONQUERS ALL OBSTACLES | LOVE TRIUMPHS AGAINST OBSTACLES AND DEFEATS OVER OBSTACLES |
| UNITY CONQUERS DESPITE ODDS | LOVE TRIUMPHS AGAINST OBSTACLES BUT DEFEATS ALL ADVERSITY |
| UNITY DEFEATS AGAINST ODDS | LOVE TRIUMPHS AGAINST OBSTACLES BUT DEFEATS ALL OBSTACLES |
| UNITY DEFEATS ALL OPPOSITION | LOVE TRIUMPHS AGAINST OBSTACLES BUT DEFEATS EACH ADVERSITY |
| UNITY OVERCOMES AGAINST ODDS | LOVE TRIUMPHS AGAINST OBSTACLES BUT DEFEATS OVER ADVERSITY |
| UNITY OVERCOMES ALL CHALLENGES | LOVE TRIUMPHS AGAINST OBSTACLES BUT DEFEATS OVER OBSTACLES |
| UNITY OVERPOWERS ALL RESISTANCE | LOVE TRIUMPHS OVER OBSTACLES AND PREVAILS OVER ADVERSITY |
| UNITY PREVAILS AGAINST ODDS | UNITY CONQUERS ALL ADVERSITY AND TRASCENDS ALL MISFORTUNE |
| UNITY PREVAILS AMIDST ODDS | UNITY CONQUERS ALL ADVERSITY AND TRASCENDS EACH MISFORTUNE |
| UNITY PREVAILS DESPITE ODDS | UNITY CONQUERS ALL BOUNDARIES AND TRASCENDS ALL ADVERSITY |
| UNITY PREVAILS OVER ODDS | UNITY CONQUERS ALL BOUNDARIES AND TRASCENDS ALL MISFORTUNE |
| UNITY RISES ABOVE ALL OBSTACLES | UNITY CONQUERS ALL BOUNDARIES AND TRASCENDS EACH ADVERSITY |
| UNITY SUBDUES ALL DIFFICULTIES | UNITY CONQUERS ALL BOUNDARIES AND TRASCENDS EACH MISFORTUNE |
| UNITY SUCCEEDS AGAINST ODDS | UNITY CONQUERS ALL DIFFERENCES AND TRASCENDS ALL MISFORTUNE |
| UNITY SURMOUNTS ALL OBSTACLES | UNITY CONQUERS ALL OBSTACLES AND TRASCENDS ALL MISFORTUNE |
| UNITY SURPASSES AGAINST ODDS | UNITY OVERCOMES ALL OBSTACLES AND CONQUERS ALL ADVERSITY |
| UNITY TRIUMPHS AGAINST ODDS | UNITY OVERCOMES ALL OBSTACLES AND CONQUERS ALL MISFORTUNE |
| UNITY TRIUMPHS OVER BARRIERS | UNITY OVERCOMES ALL OBSTACLES AND TRASCENDS ALL ADVERSITY |
| UNITY VANQUISHES ALL HINDRANCES | UNITY OVERCOMES ALL OBSTACLES AND TRASCENDS ALL MISFORTUNE |

Table S.11: Dictionary used in Simulation 4

[illegible]